AD-757 765

GLASSY CARBONS

Edward E. Hucke

Michigan University

Prepared for :

Advanced Research Projects Agency

January 1973

010199

Semi-Annual Progress Report
for the Period June 1, 1972 to December 31, 1972

Glassy Carbons

January 1973

Sponsored by
Advanced Research Projects Agency
ARPA Order No. 1824

Department of Materials and Metallurgical Engineering

Details of illustrations in
this document may be better
studied on microfiche

GLASSY CARBONS

Semi-Annual Progress Report for the Period
June 1, 1972 to December 31, 1972

January 1973

TABLE OF CONTENTS

SUMMARY

A large number of glassy carbon samples was produced by controlled pyrolysis of furfural alcohol resins, examined for structural differences, and evaluated for physical and mechanical properties. It is concluded that glassy carbon is a family of materials whose properties can be varied over a significant range, depending both on the small scale (2-50Å) carbon structure, and the amount and distribution of porosity which may be present in substantial amounts.

The combination of availability, chemical stability, low density and high strength make glassy carbons look promising for mechanical applications, particularly at very high temperatures. In terms of strength per unit weight, glassy carbons compare favorably with the best available materials even at room temperature. Very fine pored (<100Å) glassy carbons have been produced in section thicknesses of 2 inches in processing times of six days, which significantly increases the range of potential application.

The carbon's fine structure determined by electron microscopy, electron diffraction and X-ray diffraction is not homogeneous on a size scale below 100 Angstroms. The material is paracrystalline with the crystallite size ranging from 10-100Å depending on processing, and with some very crystalline features occasionally existing in sizes up to 500Å.

A thermodynamic method has given results yielding a direct measure of the degree of order in terms of the configurational entropy and enthalpy relative to crystalline graphite.

Helium, xylene, mercury intrustion, small angle X-ray scattering, surface area analysis, and scanning electron microscopy show the pore structure of glassy carbons may be either isolated or interconnected, and in a size range from 5Å to 50 microns. Mechanical strength has an inverse relation to the pore size. The pore structure allows a decrease in density, as well as the opportunity to vary mechanical properties and provide chemical filtering and absorption appliances with substantial strength.

GLASSY CARBONS

I. Introduction

This report covers work carried out during the period June 1972 to December 1972. Results of the previous contract periods are summarized in two previous semi-annual reports.[1,2] Since various property evaluations are being carried out simultaneously, the data tables included in this report are cumulative and have been revised to reflect additional samples as well as corrected in certain instances where samples were either improperly identified or errors in data reduction occurred. Complete data tables are given in Appendix A.

Glassy carbons have already been shown to have an unusual set of properties, particularly with respect to inertness and high strength to weight ratio. These attributes, together with the ready availability and high temperature capability of carbon naturally lead to potential applications in a wide variety of extreme conditions, such as reentry shields. Aside from mechanical applications, the unusual inertness in the human body has lead to a wide variety of biomedical applications, while its electrical properties have shown experimental promise as a semi-conductor switch, and its molecular sieve properties suggest applications in chemical separations.

Glassy carbon is still a new material and at present is

costly and available only in thin sections. The high cost and
section limitation both stem from the need to use very long
pyrolysis cycles in order to obtain material without cracks.
A major objective of this research has been to achieve larger
section bodies with rapid processing times.

While all of the glassy carbons made from a variety of
polymers and gaseous precursors are hard, strong and light,
many subtle variations exist and considerable tailoring of
properties is possible. A major difficulty in comparing the
various carbon materials is that no simple criteria are avail-
able to distinguish one from the other. In general, many of
the physical and mechanical properties show significant differ-
ences and one can give a comparison of one material with another
only by specifying a complete property set. All of the properties
derive ultimately from the structure and therefore it is important
to be able to elucidate, control, and specify the structure of
the material. The lack of a well-defined crystalline structure
severely complicates matters since not only are the usual micro-
structural features (.1 to 100 microns) important, but also
variations in the ultrastructure (3 to 100 Angstroms) are en-
countered. Even a seemingly straight-forward property such as
real density becomes elusive because it can vary on size scale
of the order of 50$\overset{o}{A}$.

With an understanding of structural variations possible,
extension in the range of properties achievable can be made.
From data previously available in the literature and the early

-2-

results of this program[2], it has become obvious that "glassy carbon" is not a single material, since even though it contains essentially only carbon atoms, its structure can be varied at all size levels. It seems more appropriate to think of glassy carbon as a material that may have short range atomic coordination with a variable state of crystallinity; but in addition, where rather large fractions of thermally stable voids can be arranged at size levels from 5 Angstroms to 50 microns. This accounts for the extremely wide variation in properties that can be achieved. The incorporation of voids into materials is not unique. However, it is unique to have up to 30% void remain stable in material at temperatures close to sublimation when the pore size is well below 100 Angstroms.

Glassy carbons possess some crystallinity on a scale of the order of 100 Angstroms or less, but the perfection of the crystallites is very poor by usual standards; and while the crystalline perfection may improve after heating to very high temperature, a well-defined graphitic structure is not achieved without unusual methods. The structure is better described as para-crystalline in the sense used to describe certain polymers. In fact, the glassy carbon structures are best considered polymers with vanishing contents of other than carbon atoms. The carbon structures are related to the polymer structures from which they evolve during pyrolysis. This observation follows from the differences obtainable in structure and properties of carbons after heating to 3000°C by merely changing the thermal history

of the polymer in a temperature range below 100°C where polymer structure is being formed. Thus, even though most of the atoms present in the precursor polymer are later removed, the resulting carbon inherits part of the structure.

The present study is largely concerned with structures obtainable together with the simultaneous measurement of certain key physical and mechanical properties. It is desired to achieve in different samples as wide a variation in structure and properties as possible.

The structure is being investigated from the viewpoints of the solid structure and the pore structure, which of course are related. Since significant differences can be induced in both over a size range of more than four orders of magnitude, no single technique is sufficient. Instead, combined techniques must be used. Each is discussed in detail in the following sections of the report. Representative property measurements are being carried out in conjunction with the structural examinations.

Due to the large number of samples processed, complete structural and property evaluations are not attempted on every sample. Apparent density, real density, wide angle X-ray diffraction, scanning electron microscopy, and strength measurements are made on every suitable sample. Small angle X-ray scattering, selected area electron diffraction, transmission electron microscopy, thermodynamic analysis, surface area analysis, mercury porosimetry, electrical resistivity, hardness, modulus of elasticity, and internal friction are carried out on a selected

-4-

small number of samples.

II.   Materials Preparation

During this report period over 500 samples of glassy carbon were prepared with over 95 different processing conditions. The work has continued to concentrate on furfural alcohol and a furfural alcohol resin, Durez 16470* as the carbon yielding material, with para-toluene sulfonic acid (PTSA) as the polymerization catalyst. However, a limited number of samples has been prepared with other type resins (Varcum 8051 and 4048)** and other catalysts made experimentally by the Quaker Oats Company. While glassy carbons are obtained in all cases, the yield of good material and response varies for each system. Thus far, the best results have been obtained with the Durez-PTSA system, although this may be only due to the greater experience with this system.

Catalyst levels from 2 to 20% by weight based on the monomer or resin content have been explored. Temperatures for addition of the catalyst and subsequent curing time and temperatures have been varied from several minutes to several weeks with temperatures from -11°C to 150°C. In all cases where a particularly interesting set of properties has been found, a duplicate set of specimens has been made to check reproducibility. In general, reproducibility is fair, but only if meticulous care is exercised to exactly reproduce all conditions. Standard sample cylinders

---

* Hooker Chemical Company, North Tonowanda, New York
**Reichhold Chemical Company, White Plains, New York

-5-

approximately 3 cm in diameter and 20 cm in length have been adopted. Samples up to 15 cm in diameter have been produced from coarser pored material, while a few samples of 5 cm have been made from very fine pored (<100Å) material. The latter sample is far thicker than any other similar material previously reported even though its pyrolysis time of 6 days is much shorter than usual commercial practice.

The yield of crack free material has continued to improve due mainly to increased care in catalyst addition and prevention of trapped bubbles prior to and during casting. The presence of bubbles has been found to cause cracking in the subsequent pyrolysis of the samples. In most cases, it has been possible to perform a reduced pressure de-bubbling operation after addition of the catalyst.

In order to yield good material, it has been necessary to perform the hardening of the resin systems with a minimum temperature gradient throughout the piece, which often requires cooling after addition of the catalyst. The length of time curing, curing temperature and catalyst level have been varied over wide ranges.

The single-most important factor in obtaining crack free materials in pyrolysis is obtaining a uniform slow heating rate. While heating rates have been varied from 5 to 50°C per hour in the range of room temperature to 1000°C, the yield of crack free material is much greater at the slower rates. Rates up to 200°C per hour appear to cause no difficulty in heating material previously pyrolyzed to at least 700°C. Both flowing nitrogen and

reduced pressure pyrolysis have been employed. Thus far, flowing nitrogen appears to yield less difficulty with respect to cracking.

On selected samples, carbon recovery and shrinkage data have been gathered. In both cases the data are comparable with those of the literature, namely a carbon recovery based on the total resin weight of about 55% and linear shrinkage of about 29%. However, differences in both shrinkage and recovery of about 10% can be noticed with varying of curing and pyrolysis schedule.

Inhomogeneities of about 1μ in diameter in the starting resin were noted in the previous report[2]. These regions carry through the pyrolysis and cause non-uniformity in the final structure. At present no completely satisfactory method has been found for eliminating this problem, although filtering the starting resin has made an improvement.

Rather subtle differences exist in the cured resins which result in different properties after pyrolysis. Thus far no satisfactory means for quantitatively studying the resin have been developed. Exploratory work using scanning calorimetry has been initiated in an effort to see if the differing final results can be detected from the thermal changes occuring in the polymer stages.

The single-most important processing variable is the maximum pyrolysis temperature (HTT) which has long been known to affect the structure and properties. However, all the other processing variables have some influence even though at this time the data show no clear-cut correlations. Part of the difficulty

in finding a correlation is undoubtedly due to the fact that the exothermic polymerization causes heating of parts of the sample above the temperatures of intended control. It is also probable that many of the effects noted in mechanical properties may be due to the existence of very fine cracks or possibly residual macroscopic stresses in specimens that appear to be macroscopically sound. In this case, a particular processing change may appear to cause a large effect on the properties, but may only aid in yielding a more flaw free sample. However, it is difficult for example, to understand how this explanation can be applied to the observed differences of 20% in real density (-325 mesh powder) with different curing schedules.

III.   Structural Studies

While the eventual goal of this study is to correlate structure at various stages of the process with properties, the results thus far are largely drawn from samples taken at only two processing stages. The first stage corresponds to a maximum temperature exposure in the range 650-1000°C, while the second stage is that formed at about 2000°C. More recently, samples have been examined at HTT between 1000°C and 2300°C, since for given processing conditions maximum values of mechanical proper-ties were noted in this range.

The techniques chosen for structural examination fall into two broad categories with respect to the information yielded. The first yields information predominantly about the state of the

solid making up of the structure, while the second deals mainly with the void structure. In the first category this study is employing bright field and dark field transmission electron microscopy, electron diffraction, wide angle X-ray diffraction and scanning and electron microscopy. The last two methods also yield information on pore structure.

Additional techniques used to establish the pore structure are small angle X-ray scattering, helium pycnometry, mercury porosimetry, and surface adsorption.

An attempt is also being made to gain structural information through a precise measurement of the thermodynamics of the equilibrium

$$C_{graphite} = C_{glassy}$$

Since the effort required to carry out the above techniques varies substantially, a complete set of data will be collected on only a limited number of samples after screening with more routine tests.

A. Solid Structure

X-ray Studies

Several useful measures of the state of non-graphitizing carbons can be derived from wide angle X-ray diffraction. The usual data for $d(002)$, L_c, $d(10)$, and L_a have been measured for a sample from each processing condition with the results reported in Table 1 of the appendix. The procedures are the same as previously reported[2]. The "crystallite size" parameters, L_c

and L_a are in reality only line broadening parameters and can not be literally interpreted as the size of graphite crystals, since the analysis considers only size broadening of highly crystalline material and ignores strain effects and the possibility of a distribution of layer spacings. These parameters are useful for comparing different samples of glassy carbon and correspond roughly to a paracrystalline size determined by electron diffraction.

The results obtained to date are similar to others in that they show an increasing L_c and L_a, and decreasing $d(002)$ as the pyrolysis temperature is raised. These results are consistent with the idea that the structure is based on imperfect layers from 15 to 50 Angstroms thick with a layer spacing significantly larger than graphite ($3.35\overset{o}{A}$).

As previously reported, a large number of samples, but not all, show multiple reflections within the (002) line giving the impression of a multiple phase material. These samples have been designated as 2P, 3P or NVS in Table 1 where other than a smooth broad 002 peak exists. These results give strong support for the behavior postulated by Houska and Warren[3] for carbon blacks where they concluded nearest-neighbor pairs of layers assume the ordered graphite relation independently. Layer spacings of $3.35\overset{o}{A}$ and $3.44\overset{o}{A}$ exist corresponding to ordered and disordered pairs, respectively. In the present study the 2P or 3P samples show very good agreement with these values. There is a strong tendency toward multiple reflections with higher pyrolysis tem-

perature, and some correlation with longer curing times and higher catalyst concentration. However, there are many reversals and no satisfactory reason can now be offered to explain why this behavior is sometimes present and sometimes not. It is possible that sharp lines are always present in the (002) but that their intensity is too low to allow resolution in all but exceptional cases. The electron diffraction results confirm this finding.

The only clear-cut correlation between the X-ray data and any processing variable or measured property exists with HTT. While additional correlations may be possible, it appears at present that the X-ray data are not very sensitive indicators of the structural differences that influence the measured properties. The table below indicates the relation of L_c to pyrolysis temperature.

HTT °C	Lc, Angstroms
700	15-18
1300-1450	18-26
1500-1700	19-29
2000-2300	25-110

However, for a given HTT, a variation outside the experimental uncertainty exists for samples with no other apparent processing differences.

Electron Microscopy and Diffraction

Transmission electron microscopy (TEM) is being used to examine the microstructure of selected glassy carbon samples.

Samples for direct TEM and selected area electron diffraction
(SAED) are prepared essentially the same way reported earlier[1,2],
except that now ultrasonic treatment of powder is done for 5-10
minutes. This results in smaller particles which result in better
micrographs. However, further improvements in the method of sample
preparation are still being explored.

Bright field electron micrograph obtained at magnifications
of 36400 to 66300 revealed similar structural features to those
reported previously. However, in many samples cylindrical features
and evidence for oriented texture have been seen. In general,
irregularly shaped platelets 150-500Å in diameter were observed.
The granular texture is more distinct in samples heat treated at
higher temperatures in agreement with earlier findings. There is
considerable variation in the size of platelets and granular
texture within the same sample. The characteristic platelet and
granular texture diameters are listed in Table 2.

Figure 1a, taken from sample 321-31D(2300) shows granular
texture very clearly but the platelets are not very distinct.
Similar features are also visible in certain parts of Fig. 2 taken
from sample 317-48(2000). The granular texture size recorded in
Table 2 is generally more than 'Lc', the crystallite height, and
less than 'La', the crystallite diameter, as measured by X-ray
broadening. This suggests that the texture represents domains
of paracrystalline material. The variation of size of the granular
texture is in agreement with the fact that the Lc and the La ob-
tained from X-ray line broadening are only average values of

Figure la.   Sample 321-31D(2300).   Typical granular texture
characteristic of bulk of the material.   The
platelets are not very distinct.

Figure lb.   SAED pattern from upper left corner of the above.
Both (002) and (100) contains small spots.
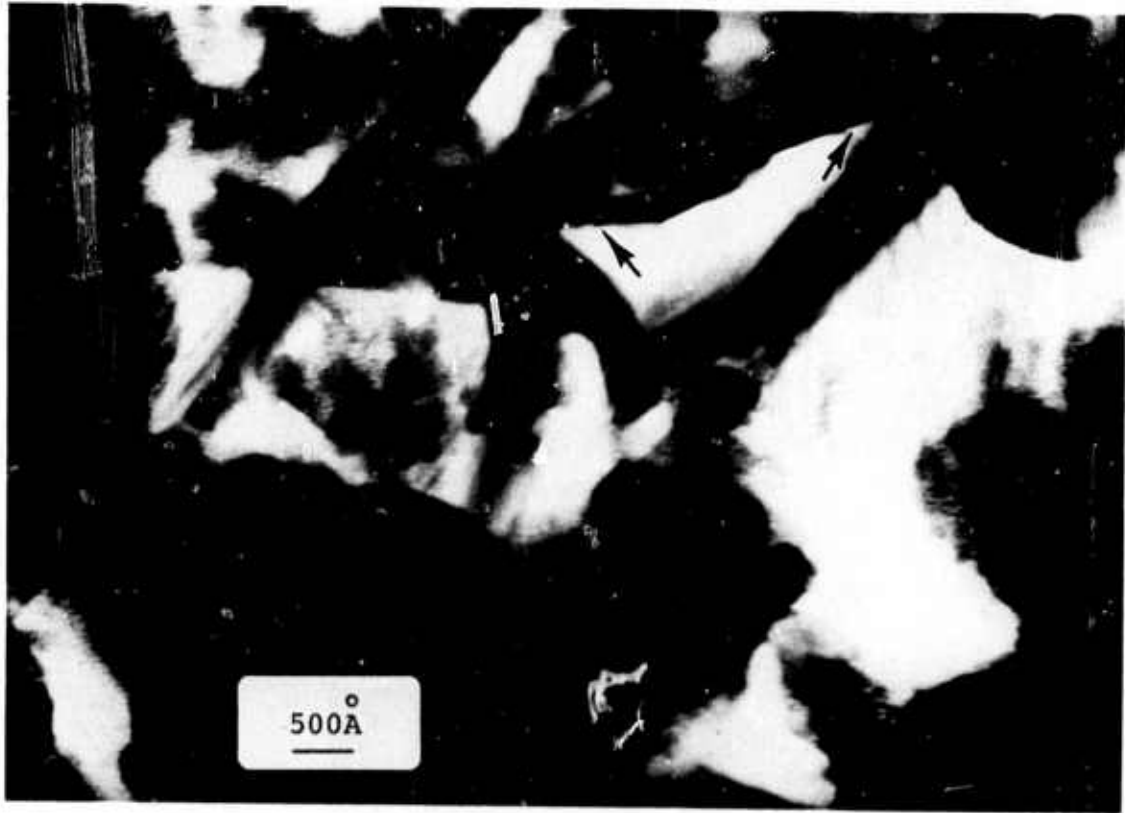
Figure 2.   Sample 317-48(2000).   Typical platelet and granular
features are shown.   In addition, cylindrical features
are also shown by arrows.

-14-

Figure 3a.   SAED from 317-49(2000).   Streaking can be seen in
             (100) and (110) halos indicating oriented texture
             (pattern was exposed thrice to bring out different
             rings and streaks).

Figure 3b.   SAED from 321-31C(2300).   Elliptical diffraction
             pattern characteristic of oriented texture.   (002)
             planes are inclined at an angle of 20 degrees from
             the beam.
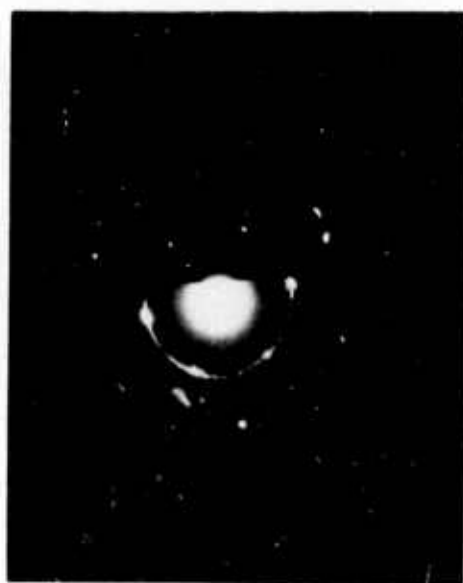
Figure 4. 321-31C(2300). (a) Very small granular texture can be seen on the upper right corner. SAED from this was typical of amorphous material. The region on the left side of the figure is more transparent and smooth. SAED of this region revealed that it is mainly graphite as shown in (b).
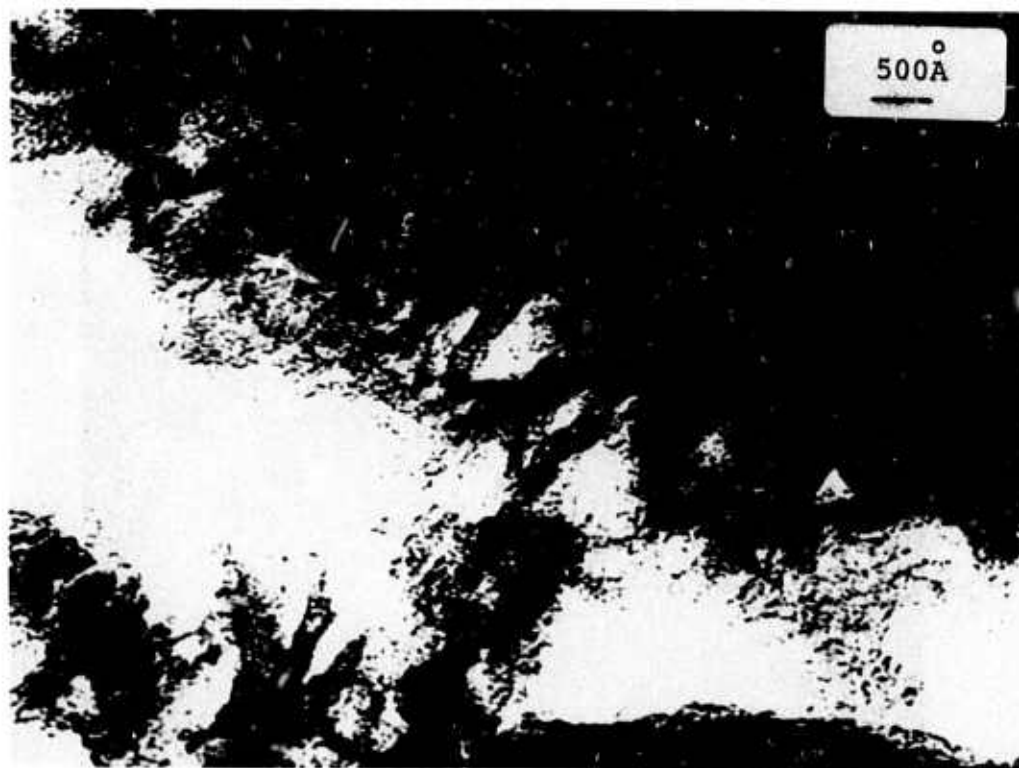
(a)

(b)
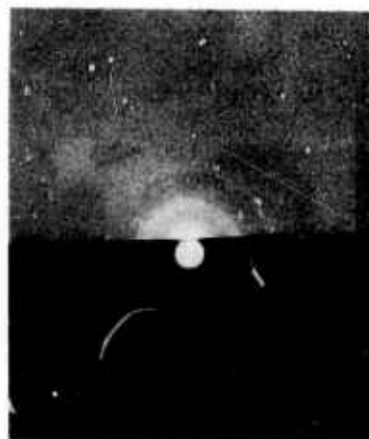
(c)

Figure 5. (a) Sample 317-48(2000). Typical granular texture
is clearly visible. However, platelets are not
present at all. (b) Selected area of (a) from which
the SAED of (c) was taken.
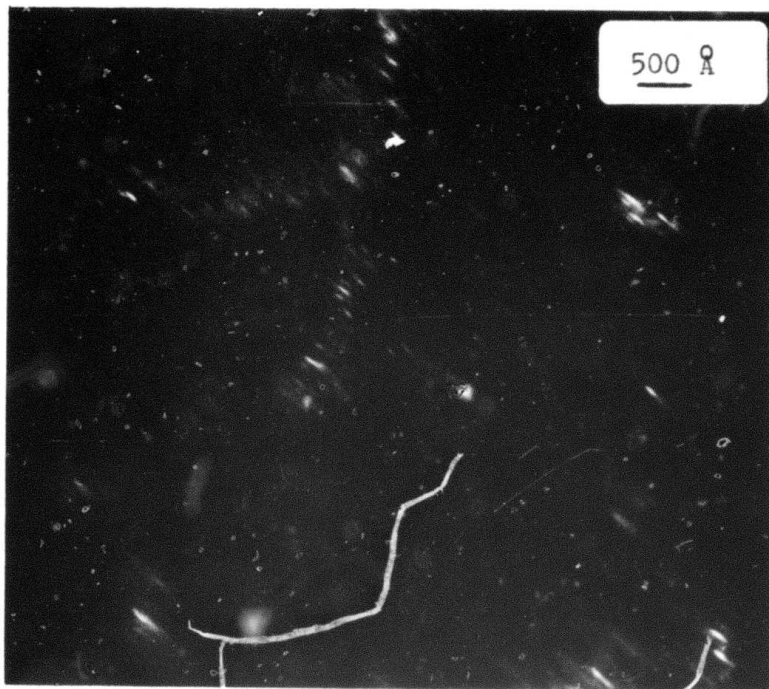
Figure 6. Sample (321-31D(2300). Dark field micrograph taken from (002) halo of SAED shown in Fig. 3b.

-18-

crystallite size and considerable variation might be present.

In some regions granular texture is extremely small and thus not very distinct. Micrograph of one such region is shown in Fig. 4a. These regions are generally highly crystalline as indicated by their corresponding SAED patterns. Fig. 4b is an example which was taken from the left side of Fig. 4a. The (002) ring of this pattern is very weak in intensity and spotty, suggesting that the basal planes are perpendicular to electron beam in most of the region. The d(002) of the region is 3.35 indicating presence of graphite crystals in the region.

Another exceptional feature reported earlier for 318-29 (2000) and 311-19(750)[2] has also been observed in the samples 317-48(2000), 317-49(2000) and 321-31C(2000). In these samples long cylindrical features are clearly visible as can be seen in Fig. 2 (indicated by arrows).

Selected area electron diffraction patterns, in most of the cases, showed three diffraction rings corresponding to (002), (100) and (110) reflection (see Fig. 1b and 5c). However, in some cases many additional rings corresponding to higher reflections were also present. The sharpness of the diffraction pattern varied from area to area within the sample. This indicates that a particular sample is non-homogeneous on a microscopic level as would be expected for paracrystalline material.

In addition to the diffraction rings, some of the diffraction patterns contained diffraction spots on the rings (see Fig. 1b and 4b). In some cases diffraction spots were slightly

-19-

displaced from the rings corresponding to smaller d(002). The presence of spots on the rings suggests that larger crystals are present in that particular area; while spots corresponding to smaller d(002) suggest the presence of more perfect crystals. These crystals have d(002) greater than 3.35Å which indicates that they might correspond to the second phase seen by X-ray diffraction. Figure 4b shows the diffraction pattern from 321-31C(2300). The area from which this is taken is very graphitic as suggested by the d(002) which is 3.35Å and six spots on the (100) ring. The (002) ring consists of very small spots of low intensity while the (100) ring is very sharp as would be expected if most of the crystals were oriented with basal planes perpendicular to the beam.

Figure 3a shows SAED pattern from 317-49(2000). The (100) and (110) rings contain "streaking", i.e., tangential straight lines on these rings. The streaking is caused by the crystals oriented with their (002) planes parallel to the beam.[4,5] Figure 3b shows elliptical diffraction patterns from (100) and (110) reflections. However, the (002) reflection gave a circular halo but cannot be seen in the figure due to its very low intensity. The distribution of reflections along ellipses is characteristic of an oriented material struck by a beam at an angle to some well-developed plane.[5] In the above case, the (002) planes are tilted at an angle of about 20 degrees from the beam.

Electron diffraction spots on the SAED patterns have also been observed in 312-31(2000) which was originally identified to

be single phase according to X-ray diffraction study. This suggests that the so-called single phase type samples may contain other phases, though in minute amounts. However, no spots were detected in sample 321-31D(2300) which was also identified as a single phase type from X-ray study. In general, 3-phase type samples show more diffraction spots and more crystalline areas compared to other types. This was seen clearly in samples 317-33 (2000), 317-48(2000), 317-49(2000), 318-12(2000), and 321-31C (2300), which were 3-phase type, and 312-31(2000) and 321-31D (2300), which were single phase type.

Ultrasonic treatment of samples before depositing them on the microgrid has resulted in better dark field micrographs from (002) reflections and made it possible to get some micrographs from the (100) reflections as well. However, dark field micrographs from the (100) ring is usually extremely poor in intensity requiring high exposure times.

Dark field micrographs, obtained from (002) reflection, reveal as bright spots the regions or crystallites giving rise to the reflection. Accordingly, the diameter of these spots is equivalent to the crystallite height, Lc. Similarly, dark field micrographs from (100) reflection represents the crystallites giving that reflection. Thus, the diameter of the spots are equivalent to 'La'. Table 2 lists the diameter obtained from these micrographs for different samples. It can be seen that the diameter from (002) dark field is in fairly good agreement with the X-ray 'Lc'. But the diameter obtained from (100) dark field

is generally very much higher than La. A possible reason for this is drifting of the sample caused by long exposure times of up to 1 minute needed to record these micrographs. Figure 6 shows the dark field micrograph obtained from the (002) reflection from the sample 321-31D(2300).

Table 3 shows that average d(002) and d(10) spacings from SAED agree fairly well with the values obtained from X-ray diffraction. The most common error in measuring these values was perhaps varying contraction of films and thus a varying camera constant for every sample. The (100) ring of graphite powder was used to calibrate the microscope for every run. Yet a further check was made with the (100) reflection from the sample itself since ideally d(100) from the sample should always yield a value close to 2.13Å.

Often additional diffracting maxima were observed, which sometimes are not indexable. Further detailed investigation is being done to find if they are not caused by impurities in the sample. However, they may be due to one or more of the crystalline forms reported by Whittaker.[6,7]

Thermodynamics

Work has progressed in the program for direct determination of the thermodynamic properties of the following equilibria:

$$C_{graphite} = C_{glassy} \tag{1}$$

$$C_{graphite} + CO_2(g) = 2CO(g) \tag{2}$$

$$CO(g) + \tfrac{1}{2}O_2(g) = CO_2(g) \tag{3}$$

$$CO_2(g) + H_2(g) = CO(g) + H_2O(g) \tag{4}$$
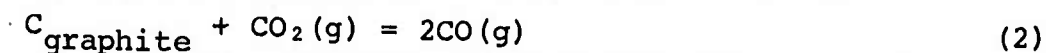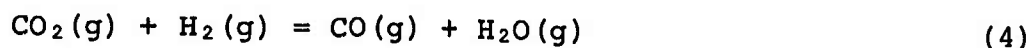
Results are available from at least one run on each of the above
equilibria. The primary interest lies in precise measurements
of reaction 1 for various types of glassy carbon, while the
others are of interest as supplements to already available data.

It has been previously noted[8,2], that values of the free
energy for reaction 1 versus temperature can be used as a direct
structural measure of the disorder of a particular carbon struc-
ture relative to graphite. Available data for the heat capacities
of graphite and various glassy carbons[9,10,11] show that any vibra-
tional contributions to the free energy in the range of tempera-
ture of interest will be 10 cal/mole or less, which is completely
negligible. Therefore, the measured differences can be considered
wholly configurational and separated into enthalpy and entropy
terms. Disorder such as mixed bonding or strained bonds will cause
changes in the configurational enthalpy and a definite increase in
the configurational entropy, which can be directly interpreted as
a numerical disorder parameter. Such techniques have already been
applied in the case of polymers to determine degree of crystall-
inity[12], where configurational (residual) entropies up to 5 cal/
mole-$^{\circ}$K are found. Configurational enthalpies of $\sim$1500 cal/mole
have been previously measured[13] between glassy carbon and graphite
by heat of combustion. Using another reaction, rather large
energy differences have also been measured[14] between graphite in

-23-

normal and rhombohedral stacking. In addition, Gordon[15] has
pointed out from an examination of the discrepancy between
experimental determinations of the equilibrium constant for the
producer gas reaction and values derived from heat of combustion
and spectroscopic data that a residual entropy of .5 cal/mole-°K
may exist in near perfect graphite. The proposed cell method
should be considerably more accurate than the previous methods
and yields both the ΔH and ΔS.

A rather extensive set of check runs has been made in
order to insure precision and otherwise check experimental
procedures. A series of runs previously reported[2] was carried
out on oxides (NiO, FeO, CoO, NbO_2, Nb_2O_5, CO_2, H_2O) with
known thermodynamic properties in order to verify cell configur-
ations, electrical and temperature measurement techniques, gas
train functioning, thermal diffusion effects, and solid electro-
lyte composition. In all cases, extremely gratifying confirm-
ations were found.

Measurements have been carried out with two entirely
different cell techniques; however, at this time, not for the
same sample. The first type uses a molten salt, $CaCl_2$ with
CaC_2 dissolved, and involves reversible transfer of carbon
directly from one electrode to the other. While the method is
straight-forward, the useable temperature range and other
experimental difficulties cause limitations. Also, the details
of the charge carrying species are less certain since only one
previous study[16] has been completed. However, Fig. 7 shows

-24-

pt/graphite/Ca C_2(Ca Cl_2)/glassy carbon/pt

$\oplus$ $\ominus$

Graphite → Glassy Carbon

Glassy Carbon

321-7-1400°C

321-7-1600°C

ΔG cal/mole

Temp. °C

Graphite

321-7-1400°C ●
ΔH = 8,909 cal/mole
ΔS = 7·45 e.u.

321-7-1600°C ▲
ΔH = 752 cal/mole
ΔS = 0·65 e.u.

Figure 7.

-25-
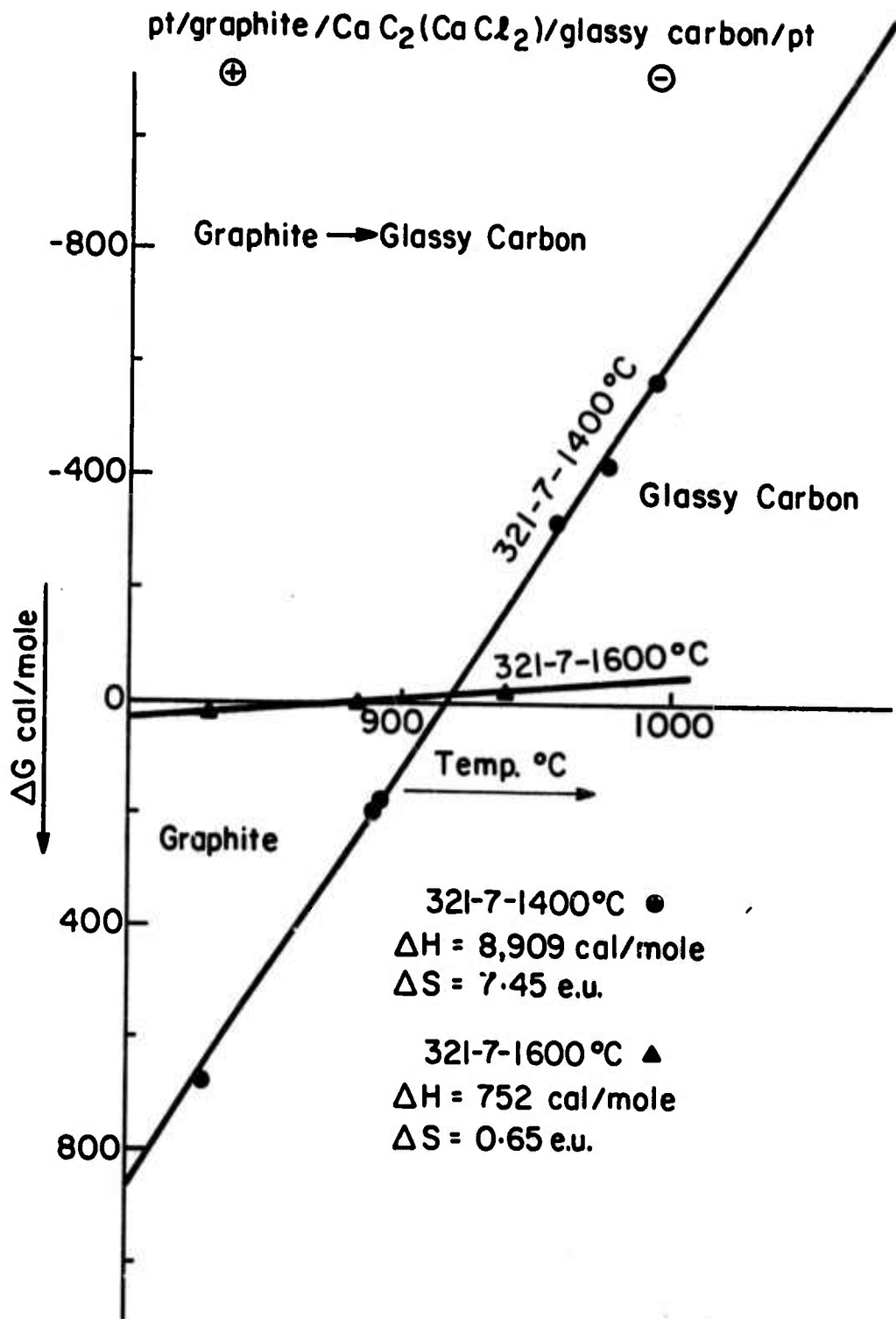
the results obtained for two portions of a glassy carbon sample differing only in the HTT, i.e., 1400°C vs. 1600°C. The data, as expected, fall on two straight lines which yield the results below

Sample	ΔH, Cal/mole	ΔS, Cal/mole-°K
321-7(1400°C)	8909	7.45
321-7(1600°C)	752	.65

The results, especially for the 1400°C sample are remarkedly high but are quite consistent with the expected behavior of less disorder after higher treatment temperatures. While this cell technique appears feasible, it will be held as an alternative and check procedure since the solid electrolyte technique seems more versatile.

The solid electrolyte cell involves measuring the difference in O_2 pressure existing of opposite sides of the electrolyte where this pressure is additionally constrained to be in equilibrium with CO and CO_2 and solid carbon. The details of analysis have been presented elsewhere.[8],[2] If a difference in P_{O_2} exists between the two sides at equilibrium with the same temperature and total pressure after starting with either CO or CO_2 or O_2, then it can only be due to a difference in the activity of the two carbons. While the equilibrium value may be the same regardless of the starting gas, the rate may be quite different. In order to check the functioning of the cell, several runs were made with Pt only on both sides and then with graphite on both

-26-

sides in order to verify that no stray EMF was involved. The cell voltages measured were always less than .1 millivolts. The graphite used in all the runs to date has been a common electro-graphite (UCC-grade CS) and will be replaced by a carefully selected graphite standard.

The cell was next run with air on one side so that the measured EMF is a direct measure of reaction 2, where the activity of the solid carbon (graphite) is unity by definition. The results are shown in Fig. 8. The agreement is extremely good, since the experimental points lie very close to the best known line and well within the scatter band for the previously available data. Even more refined measurements over a wider temperature interval will be made on the graphite standard. The cell was well-behaved with equilibrium established within several hours. Equilibrium could be approached from both directions and the same value obtained after thermal cycling. The cell voltages have been measured with a high impedance Keithley differential voltmeter, a Keithley electrometer, and a calibrated L&N potenti-ometer, purposely set to polarize the cell in opposite directions. These experiments show the cell EMF to be reproducible, sensitive, accurate, reversible, and sign consistent.

The next series utilized graphite in one compartment and various glass carbon solid discs in the other. The glass carbons are weighted for total carbon loss and both sides are exposed to pure CO_2 after evacuation. Companion runs on the same samples starting with O_2 both before and after CO_2 exposure are planned.

-27-

Figure 8.

C(s) + CO$_2$(g) = 2CO(g)
Total Pressure = 0.976 atms
pt/Air(g)/ZrO$_2$-CaO/graphite(s), CO(g), CO$_2$(g)/pt

• Present Study
— Calorimetric Data
-- Scatter Band

$\Delta G°$ cal/mole

TEMP °C
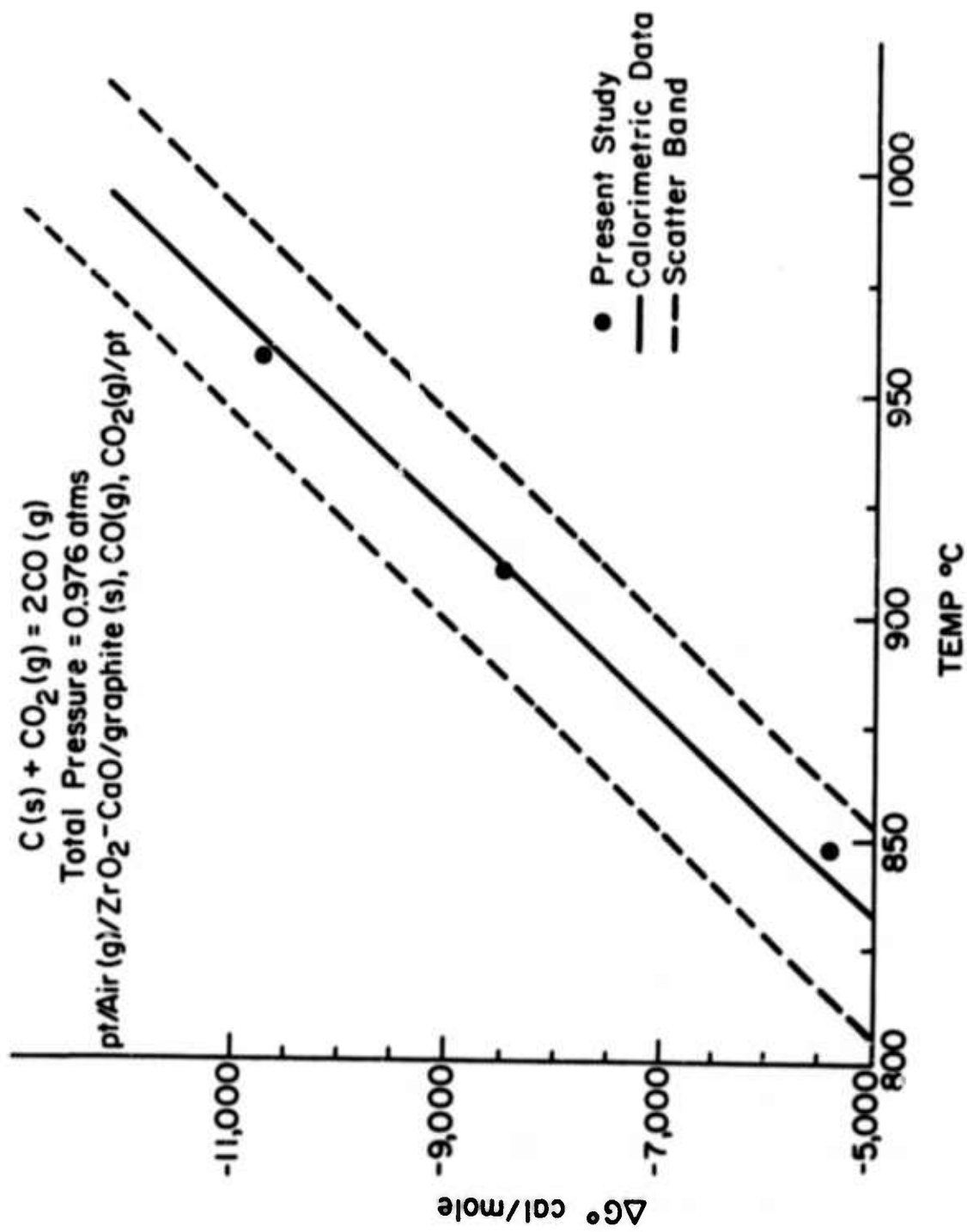
The results for portions of a glassy carbon pyrolyzed to 700°C and then vacuum heated for 1 hour to 1060°C, 1243°C, and 1800°C are given in Fig. 9. Again, as expected, the data fall on good straight lines giving the following values for ΔH and ΔS which are shown in a provisional plot in Fig. 10.

Specimen	ΔH, Cal/mole	ΔS, Cal/mole-°K
321-13(1060°C-Vac)	9029	8.66
321-13(1243°C-Vac)	4934	4.70
321-13(1800°C-Vac)	3689	4.60

The rate of approach to equilibrium at the higher temperatures was rapid, but took 2 to 3 days at 650°C, the lower limit for the electrolyte. Future runs call for use of crushed samples to hasten equilibrium. The EMF's of up to 40 millivolts were stable, sensitive, reversible and could be approached from heating or cooling. There can be no doubt that replacing graphite with glassy carbon caused a dramatic change in cell voltage.

While the data are yet too few to draw sweeping conclusions, they do show the expected trends. Again, the magnitudes are embarrassingly high. It is interesting to note that the configurational enthalpy drops steadily with HTT while the order increases rapidly from 1060°C to 1200°C, but very little from 1200°C to 1800°C. Further conclusions must await data for more samples including carbons of many different types and measurements over a larger range of temperature.

It is interesting to note that the above data can be

Figure 9.

-30-
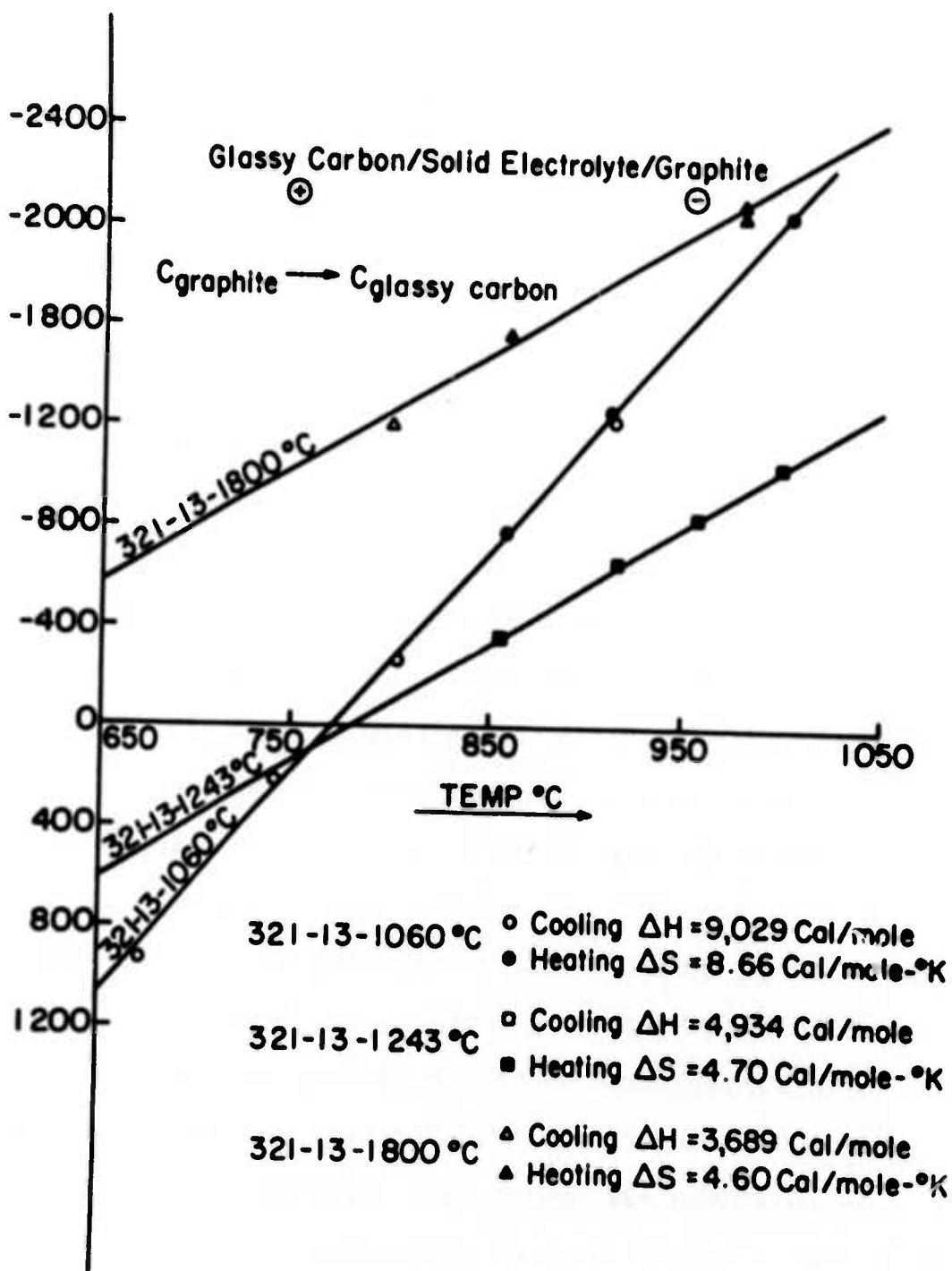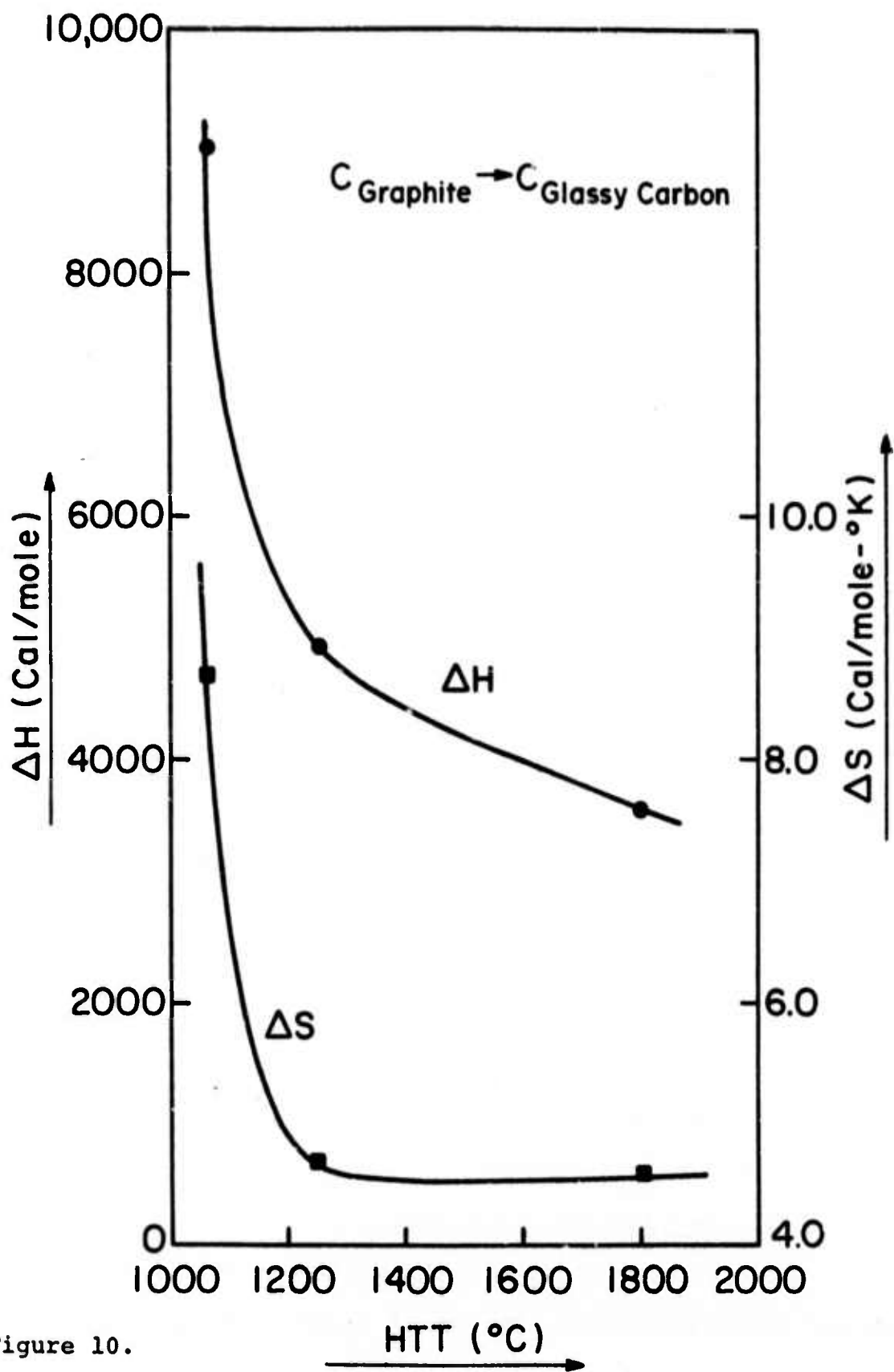
Figure 10.

used to directly calculate the ratio of carbon sites occupied by O to those free, if one uses data available for reaction 3 and for the oxygen exchange reaction[17],

$$C_O + CO(g) = CO_2(g) + C_f \qquad (5)$$

Example calculations are given below.

Temperature	Graphite $\left(\dfrac{C_O}{C_f}\right)$	Glassy Carbon 321-13(1060°C, Vac) $\left(\dfrac{C_O}{C_f}\right)$
800°C	0.0128	0.0143
1000°C	0.00458	0.01

It can be seen that the surface of glassy carbon is much better covered with oxygen than is graphite at 1000°C.

Work has progressed on a structural model for carbons allowing calculation of the entropy of disorder. At present the results are encouraging but not complete enough for presentation.

B. Pore Structure

The details of pore structure are being investigated with a variety of techniques, including small angle X-ray scattering, scanning electron microscopy, pycnometry, surface adsorption, and Hg porosimetry.

Small Angle X-ray Scattering

Microporosity is one of the main characteristics of the non-graphitizing carbons. The small angle X-ray scattering

permits the evaluation of general structural parameters if recent developments in theory are used to analyze the scattering. Perret and Ruland's[18] work on the non-graphitizing carbons gives an outstanding example. The determination of the pore size and the pore size distribution can be made using Guinier's analysis which has been performed on several samples.

For the evaluation of R_G, the Guinier radius, the approximation

$$I(S) = n^2 \exp(-\frac{4}{3} \pi^2 R_G^2 s^2)$$

is considered to be valid. Here I(s) is the observed X-ray intensity and s is 2 $\sin\theta/\lambda$, where θ and λ are the Bragg angle and wave length, respectively. The R_G can be obtained from a plot of I(s) versus s^2, which is a straight line if the distribution of particle size is narrow. Pore size can be calculated from R_G if the shape of the pores is known. If the pores are spherical then

$$a = \sqrt{\frac{5}{3}} R_G$$

where a is the radius of the pore.

The extent to which the log I(s) versus s^2 plot follows a straight line gives information about the pore size distribution. In the case of a wide distribution of pore size, the slope of the I(s) versus s^2 curve varies from point to point.

Experimental Procedure

Copper Kα radiation was employed with pinhole collimation. The intensity was collected on the photographic films. The

density of the films was measured using a Joyce-Loebl micro-densitometer. The samples in all the cases were a few milli-meters thick.

Results

Figs. 11 and 12 show results for some of the samples studied. As can be seen, most of the samples follow Guinier's law, i.e., the log I versus s^2 plot is a straight line.

Table 4 gives our values of "a" along with the reported values for some commercial samples. The agreement is not very good. As in our case, the values are almost twice the reported values. However, all three samples follow Guinier's law fairly well up to $S^2 = 2 \times 10^{-4} \overset{\circ}{A}^{-2}$ and very little polydispersity is seen which agrees very well with reported results.

Table 5 shows the "a" values for some of our samples. It has been found that samples 317-45(2000), 318-11(2000), 318-42 (2000) are not monodisperse. In these cases the pore size has been determined from the average value of the slope.

The pore size is smaller for the samples heat treated at 700°C than the samples heat treated at 2000°C. This is in agree-ment with the work of Perret and Ruland on the non-graphitizing carbons.[18]

There seems to be a strong correlation between the appear-ance of multiple reflections in the (002) line and the appear-ance of polydispersity in small angle scattering. A further in-vestigation of this point is in order.

Currently, the unit is being adjusted for the slit colli-
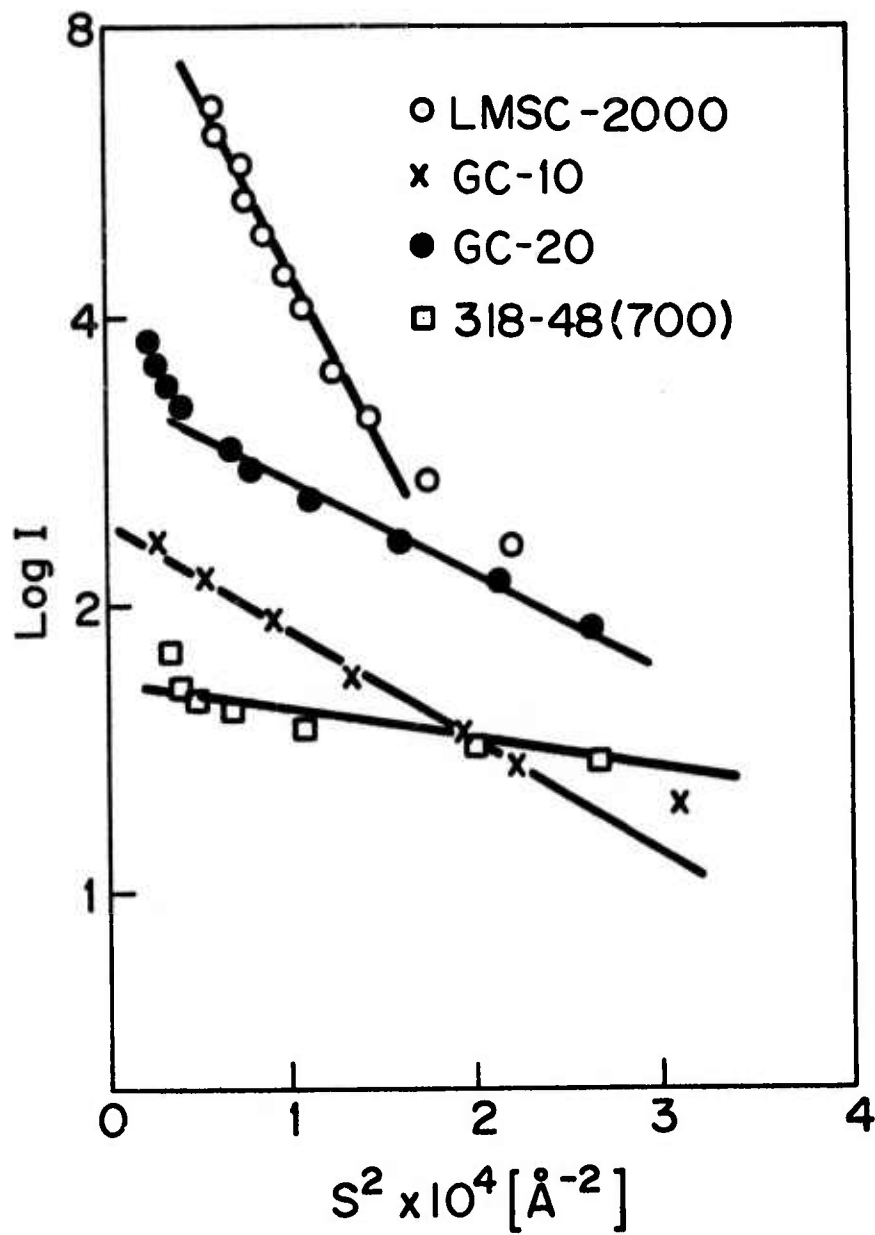
Figure 11. Guinier plots for four different samples. Intensity values are in arbitrary units.
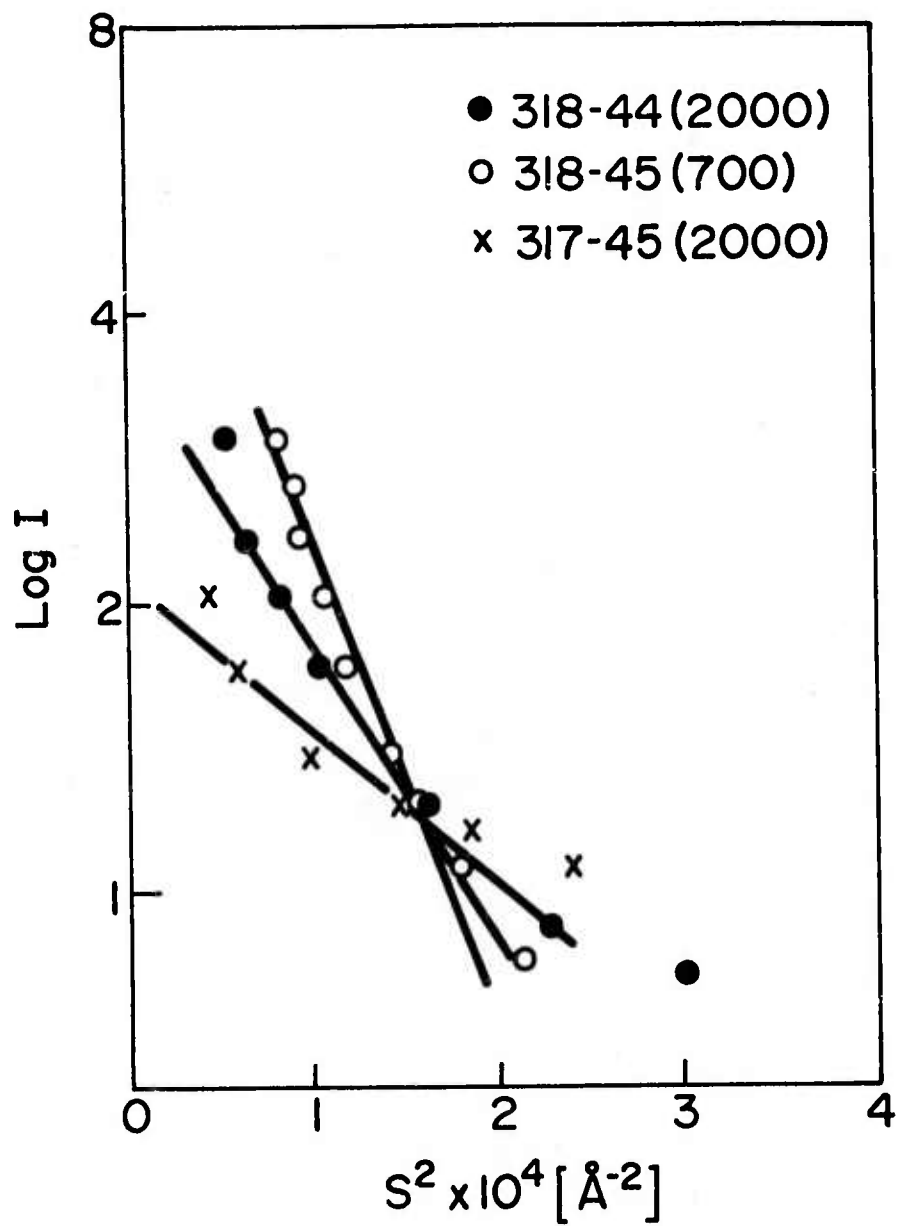
Figure 12.   Guinier plots for three different samples.
Intensity values are in arbitrary units.

mation so that a counter can be used to determine the intensity and reduce the experimental time per sample.

Electron Scanning Microscopy

Electron scanning microscopy is employed on a fracture surface of each sample to obtain additional information on the pore structure. For the coarser materials (>200Å) the pore structure is easily discernible with this method. However, for the finer materials, the size of the pores is equal to or finer than the 100Å resolving power of the instrument, rendering the determination of quantitative information impossible. Also, the SEM pictures show a surface roughness of the same order of size as the pore structure which makes pore size assessment difficult.

In many instances, it has been possible to compare the average pore size as measured with SEM to that obtained for Hg porosimetry. The agreement is satisfactory though not precise. For the finer pored materials, lack of resolving power and surface roughness preclude even a rough quantitative check. However, from the observations made on coarser materials, it may be concluded that the Hg intrusion pore diameter is approximately the same as actually seen in the microscope.

The microstructures examined show the same general features as presented previously[1,2], although some improvement in presence of foreign "agglomerate" particles has apparently resulted from filtering the starting resin.

Pycnometry

As a routine characterization of the pore volume open to He, the real density was measured in a commercial pycnometer made by Micrometrics Inc. of Norcross, Georgia. Powder samples, -325 mesh, are used routinely. Data for samples thus far measured is included in Table 8. Considerable difficulty has been encountered in the He density measurements for carbons with HTT in the range of 700°C. In this range the carbons are known to have a very large micropore volume which has been verified by our surface area determinations. Data for some of these samples yielded an apparent negative density, probably due to a rather large absorption of He in the micropores of the carbon. While in these cases it is obvious that an error exists, it may be that much of the variation in He density of other samples is caused by smaller, but variable, amounts of adsorption.[19] Many of the 700°C samples, however, behaved normally. In general, as expected with these samples, the 700°C density was higher than that at 2000°C as can be seen for example in Table 6. As a result, densities are now being measured by Xylene immersion. In most cases the Xylene density is quite reproducible, and in most cases, slightly lower than the He density as expected.

In addition to real density, the apparent density of the bulk samples is determined geometrically. Table 2 includes the results obtained to date.

Surface Area

Additional surface area data for samples 321-9 have been gathered since those in Table 6 reported previously[2]. The high surface area ($\sim$500 m^2/gm) of glassy carbons treated to 700°C was again confirmed, as was the dramatic drop after pyrolysis to 2000°C. Sample 321-9 is characterized by relatively high apparent density and very fine pore size as seen in the Hg porosimetry data of Table 7. However, the open porosity of 57 to 73Å can not be the porosity accounting for the very high surface area of the 700°C sample as can be seen by comparing the Hg data for the 700°C and 2000°C samples. While the open pore system is about the same size, the 700°C sample has slightly less intrusion pore volume, but almost 50 times the open area for nitrogen adsorption. Similarly, for sample 318-22, the slightly higher Hg intrusion pore volume gives no significantly larger nitrogen surface area. The large surface area is probably assoc-iated with the smaller pore system (5-?0Å) disclosed by small angle scattering and molecular probe techniques.

Mercury Porosimetry

Mercury porosimetry was used to determine pore size distribution, interconnected pore volume, density and median pore diameter values. Data obtained to date are shown in Table 7. In most cases, a rather sharp pore size distribution was observed, however, a few samples yielded a wide distribution. The porosi-metry data indicate that it is possible to produce material with a rather large open pore volume (up to 65%) with a pore size

-39-

ranging from 30 Angstroms to 50 microns. In addition, there is a pore structure at a smaller level of 5-15$\overset{o}{A}$ which is open in low temperature carbons to the macropore system. This allows rather exciting possibilities in providing structurally strong, inert elements that could serve both as filters and absorbers.

Higher processing temperature (HTT) closes the very fine pores and causes them to grow according to surface area and X-ray scattering results. The macropore system, even though it is very fine ($\sim 30\overset{o}{A}$) in some cases, changes relatively little up to 2000°C. In most cases, noted in Table 7, the pore size decreases slightly while the pore volume remains about constant.

IV.   Property Evaluation

Because the glassy carbons under investigation were produced under a wide range of processing variables, a large degree of variation in structure and physical properties was observed. Based on previous information, some of which was included in a previous report[2], several tests were chosen as a means of obtaining preliminary mechanical property data. The mechanical properties investigated thus far include hardness (DPH), compressive strength, ultimate tensile strength (Dimetral compression) and sonic modulus of elasticity. In addition, internal friction and electrical resistiveity were measured on selected samples.

-40-

Hardness

Hardness measurements of these materials have posed
constant problems, despite the appeal of providing a quick
mechanical measurement. At present no test has been found com-
pletely satisfactory since the various carbons vary so widely
in pore volume and pore size. The indentation in many of the
materials occurs largely by densification under the indentor.
In most cases there is a large recovery. Attempts were made
during this report period to develop a Rockwell type test which
measures depth of indentation instead of indentation stress.
Satisfactory testing could be done without cracking at rather
large loads using a 1/8" diameter ball. However, the results
on widely differing carbons failed to correlate with strength,
Vickers hardness, modulus, or scratch hardness. Further hard-
ness testing awaits development of a more relevant test.

Compressive and Ultimate Tensile Strength

Further results are reported in Table 8 and presented
on "reduced" basis in Table 9. Values were revised where
additional data warranted change.

To show the relevance of the diametral disc rupture test,
tensile bars 2 inches long by 3/8 inch diameter were ground,
threaded gripping ends epoxied in place, and tested in uniaxial
tension on an Instron. In this way, a large sample volume is
under stress. The results are given in Table 10 showing a very
gratifying agreement. The tensile data surpassed the disc
results in half the cases. A similar comparison is planned with

-41-

three point bending tests on very small samples, which normally gives unrealistically high values.

The tensile disc test often gives a stepped stress-strain curve which raised the possibility that the pores may be functioning as crack stoppers. This observation can not be definitely confirmed at this time since there is a possibility of compressive failure occurring at the disc edges due to stress concentration before the tensile strength has been exceeded in the center of the sample. However, Tingey has noted[11] definite acoustic emissions from these materials prior to catastrophic fracture indicating that the steps may indeed correspond to cracking between pores.

Various correlations have been attempted between strength properties and processing variables, apparent density, real density and pore size without great success. The raw data show a broad correlation with apparent density; with higher strength occurring at higher density. Also, a fair correlation (Figs. 13 and 14) exists with intrusion pore diameter, higher strengths with smaller pores. No other correlations are evident at this time. Since strength is controlled by fracture path, it would be determined by the maximum path within the carbon, i.e., distance between pores. For similar structures and constant densities (real and apparent), the mean free path would vary directly with the average pore size. Unfortunately, these conditions are not met between different samples and further, the only measure of the pore size over an adequate range is the mean

-42-

Figure 13.

-43-
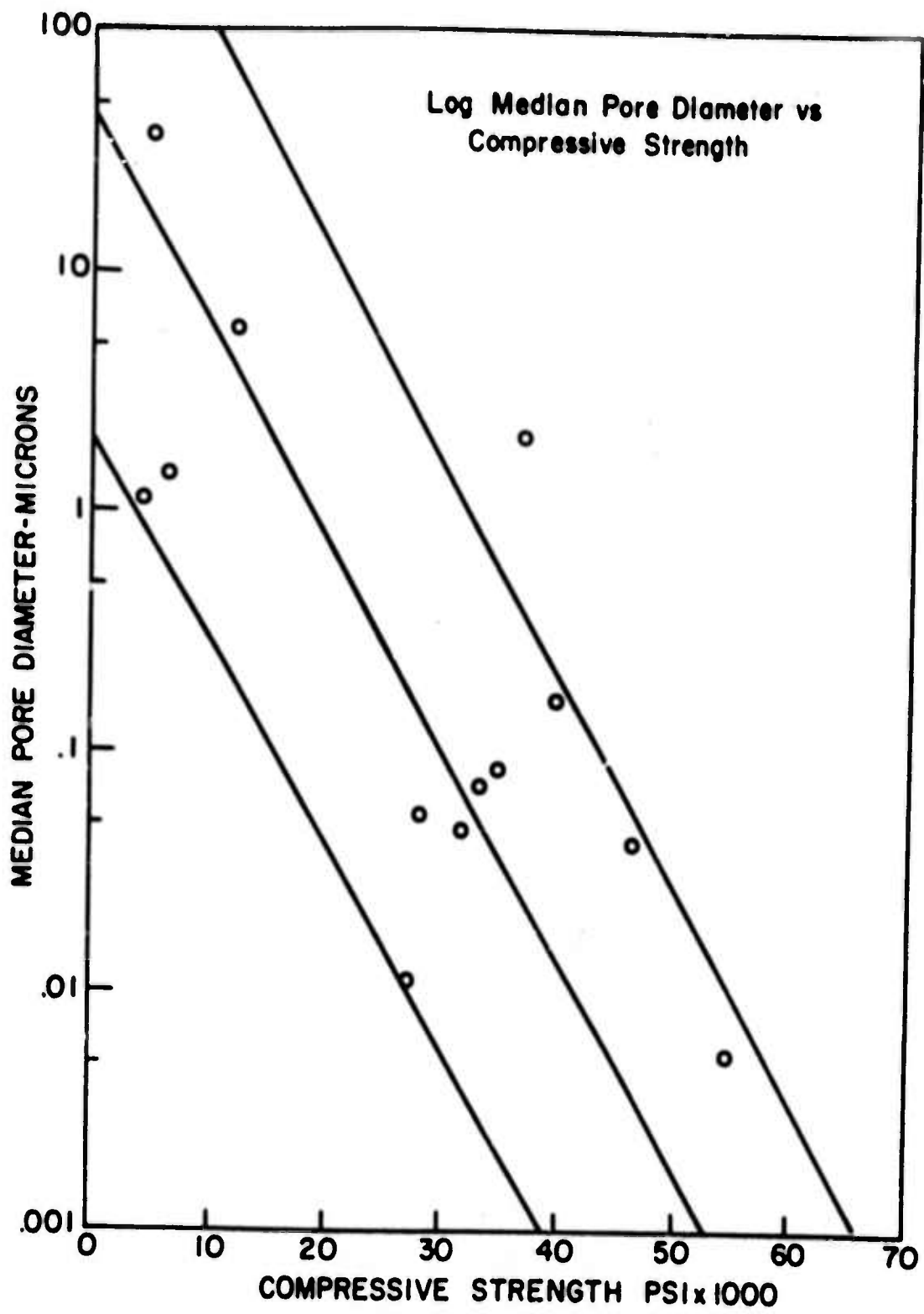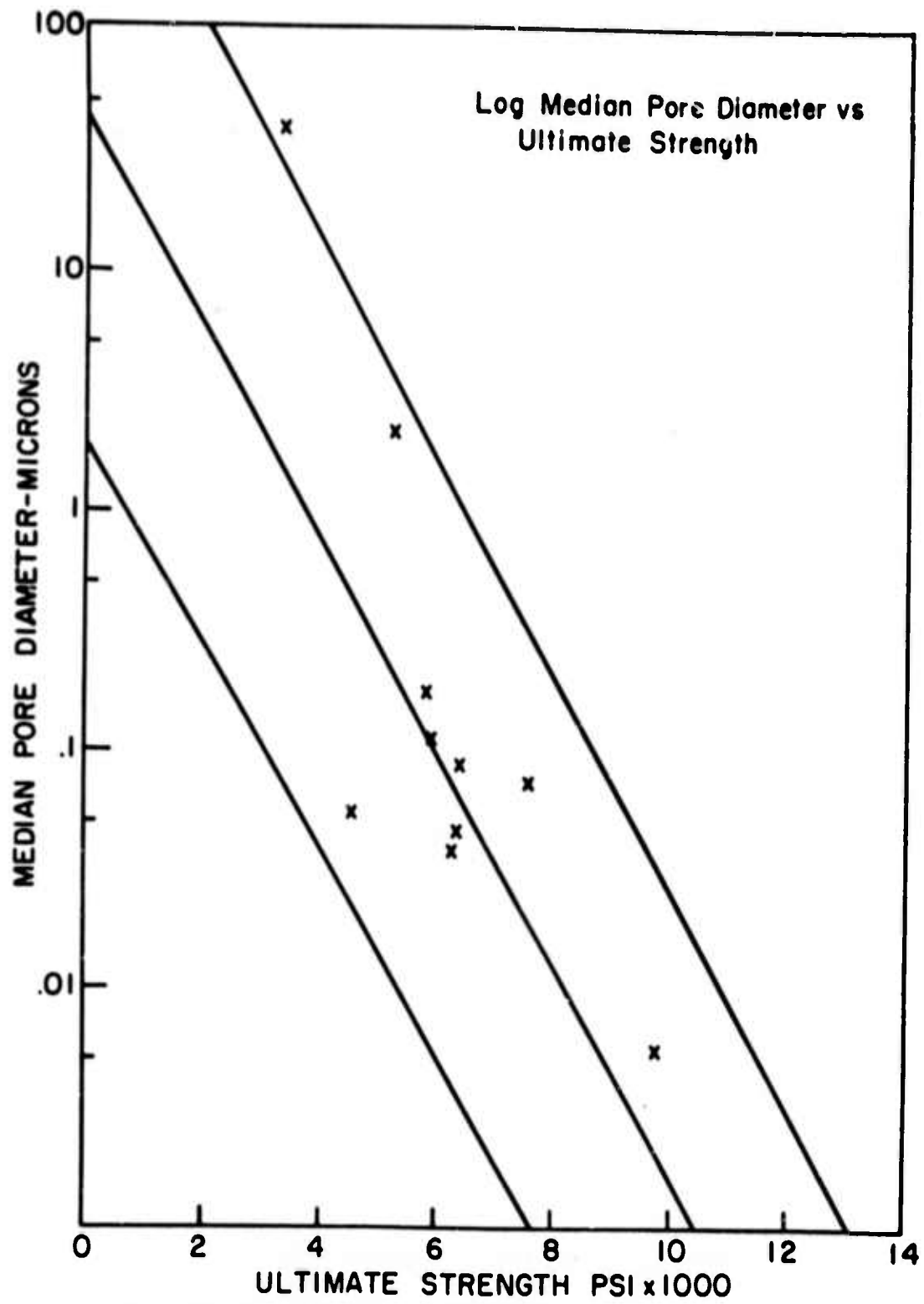
Figure 14.

intrustion pore size. Attempts to use SEM measurements are not very fruitful since the interesting range occurs at sizes where the path length is not easily measured.

The reduced data shown in Table 9 show less range than the raw data. As one method of data reduction, the various mechanical properties are divided by density to yield value of specific strength. On a specific basis these carbon materials compare very favorably with the best available structural materials. Considering the high temperature capability of carbon, the comparison becomes even more favorable.

In addition, the area dependent properties have been normalized by either multiplying or dividing by the area fraction carbon, which is proportional to the volume fraction unavailable to He (i.e., ρ_a/ρ_{He}), assuming all pores open to He. It can be seen that this normalization considerably reduces the range of values exhibited by the various carbons. However, since the compressive and tensile strengths are certainly dependent on macrostructure as well as fine scale binding of carbon atoms, some range of reduced properties is to be expected.

Sonic Modulus and Internal Friction

A conversion factor error was noted in the modulus data presented in the last report[2]. All data subject to this error have been recalculated reducing the previous results by a factor of .75. However, the extremely wide range possible in porous glassy carbons is still present, i.e., from $.35 \times 10^6$ psi to 5.8×10^6 psi. When the data are reduced to reflect the volume

fraction carbon, the range goes from $.32 \times 10^6$ psi to 10.06×10^6 psi, with most samples falling around 2.5×10^6 psi. This value is reasonably close to that reported for other more dense glassy carbons. However, the existence of such a wide range is quite interesting since the modulus should not be very dependent upon gross microstructure, but should be determined by shorter range carbon-carbon bonding.

In order to determine whether the sonic modulus, which involves very small strains, well approximates the mechanical modulus, test bars were fitted with strain gages. Prior calculation had already justified that the difference between adiabatic and isothermal moduli for these materials should be negligible. Table 11 shows a comparison of results, which indeed shows that the sonic modulus is a good measure of the modulus at higher strains.

The modulus data versus HTT are shown in Table 12. In all samples the modulus rises from about 10^4 psi after low temperature curing to about 10^6 psi after 700°C HTT and then passes through a broad maximum ($\sim 3 \times 10^6$ psi) between 900-1500°C HTT. The HTT for this maximum for a single sample series will be investigated including some temperatures below 700°C.

The rather remarkable increase in modulus between the cured and pyrolyzed states illustrated below warrants further study. The evolution of the stiffness with curing may be useful in sensing changes in "crosslinking" in a given sample and between

-46-

samples if a suitable method can be devised for normalizing the
data with respect to structural changes.

Sonic Modulus, psi

Sample Treatment Temperature °C

Sample	70°C	95°C	700°C
318-35	--	1.52×10^4	$.76 \times 10^6$
318-36	--	2.47×10^4	1.2×10^6
318-37	--	1.56×10^4	$.69 \times 10^6$
318-39	$.74 \times 10^4$	--	$.9 \times 10^6$
318-45	5.5×10^4	--	1.09×10^6
318-46	6.2×10^4	--	$.89 \times 10^6$

Internal friction measurements have been discontinued
for the present. While remarkable differences in behavior of
the various samples have been noted, no straightforward method
of correlating these changes to structure has been developed.
The anomalous decay curves found in some samples earlier[2] are
believed to be associated with mixed frequency excitation due
to the specimen claiming device rather than related to porosity
as first thought.

Resistivity

Refinements of the measuring set-up have allowed more
accurate measurements, particularly at low resistivity. Cumu-
lative data is presented in Table 13. Resistivity will be
continued on a limited basis, especially as a parallel check
of sonic modulus data for the low temperature development of
crosslinking.

It is interesting to note that the resistivity of

nearly all samples on a reduced basis falls between 10^{-3}-10^{-4} Ω-cm which is the same as for other glassy carbon materials pyrolyzed to 2000°C.

REFERENCES

1. E. E. Hucke, "Glassy Carbons," Semi-Annual Report, January 1972, Contract No. DAHC15-71-C-0283.

2. Ibid, June 1972.

3. C. R. Houska and B. E. Warren, J. Appl. Phys. 25, (1954).

4. D. Kay, *Techniques of Electron Microscopy*, Blackwell Scientific Publications, Oxford Press, 1967.

5. B. K. Vainshtein, *Structure Analysis by Electron Diffraction*, MacMillan, New York, 1964.

6. A. G. Whittaker and P. L. Kinter, Science 165, 589 (1969).

7. A. G. Whittaker and B. L. Tooper, "Single Crystal Diffraction Patterns from Vitreous Carbon," to be published.

8. E. E. Hucke and S. K. Das, "A Proposed Method for the Evaluation of the Thermodynamic Properties of the Glassy Carbon-Graphite Equilibrium," Preliminary Reports, Memoranda and Technical Notes of the ARPA Materials Summer Conference, July 1971, Contract No. DAHC15-71-C-0253.

9. Y. Takahashi and E. F. Westrum, Jr., J. Chem. Thermo. 2, 847 (1970).

10. J. Yokoyama, M. Murabayashi, Y. Takahashi, T. Mukaibo, Tanso 65, 44 (1971). (Translated from Japanese.)

11. G. L. Tingey, Semi-Annual Technical Report for the Period 2 Nov 71 to 1 May 72, "Investigation of the Influence of Structure on Chemical Stability and Thermal Mechanical Shock Properties of Glass-Like Carbon," Battelle-Northwest Labs., Richland, Washington, June 1972.

12. M. C. Shen and A. Eisenberg, Rubber Chemistry and Technology 43, 95 (1970).

13. J. B. Lewis, R. Murdock and A. N. Moul, Nature 221, 1137 (1969).

14. H. P. Boehm and R. W. Coughlin, Carbon 2, 1 (1964).

15. A. R. Gordon, J. Chem. Phys. 1, 308 (1933).

16. G. L. Hawkes and D. R. Morris, Trans. TMS-AIME 242, 1083 (1968).

17. S. Ergun and M. Mentser, *Chemistry and Physics of Carbon*, Vol. 1, p. 203, Marcel Dekker, Inc., New York, 1965.

18. R. Perret and W. Ruland, J. Appl. Cryst. $\underline{1}$, 308 (1968).

19. K. A. Kini and W. O. Stacy, Carbon $\underline{1}$, 17-24 (1963).

APPENDIX

TABLE 1   SUMMARY OF X-RAY DATA

(All values in Angstroms)

Symbols Used in the Tables

Experimental Condition

All the samples were run in a Phillips-Norelco Diffractometer using CuKα radiation under the following conditions:

Tube Voltage: 45KV
Tube Current: 14mA
Proportional Counter Voltage: 1.622KV
Proportional Counter Time Constant: 4 sec.
Chart Speed: 1/2 inch/min.
Scan Speed: 1.2 degree (2θ)/min.
Slits: 1°/006"/1° at Primary/Scattering/Secondary

Sample used of thickness of 3mm in all cases except where otherwise designated. The value of d(10) refers to the unresolved (100) and (101) peak.

(002) Peak Type

S: "Smooth" (or single phase) Peak
NVS: "Not Very Smooth" Peak
2P: "2 Phase" Peak
3P: "3 Phase" Peak

Sample Designation	Temp. (°C)	(002) Peak Type	d(002)	Lc	d(10)	La
Graphite, solid 3mm & 1mm thick		S	3.37	Very High	2.13	Very High
Graphite		S	3.37	Very High	2.13	Very High
Graphite, natural (Reported)		S	3.35	Very High	2.13	Very High
Graphite, synthetic (Reported)		S	3.37	Very High	2.13	Very High

Sample Designation	Temp. (°C)	(002) Peak Type	d(002)	Lc	d(10)	La
Commercial Samples						
Lockheed, solid	2000	S	3.53	21.2	2.09	98.0
Lockheed, reported	2000		3.56	19.0	--	--
Beckwith, solid	2000	S	3.55	23.2	2.09	112.0
Beckwith, reported	2000		3.54	15.0	--	50.0
Tokai, solid	1000	S	3.70	14.2	2.07	43.7
Tokai, reported	2000		--	--	--	--
Atomergic Chemicals Co., V-25, solid	2500	S	3.52	30.2	2.09	66.0
Atomergic Chemicals Co., V-25, reported	2500					
Atomergic Chemicals Co., V-10	1000	NVS	3.44	45.0	2.10	70.0
Atomergic Chemicals Co., V-10, reported	1000		--	--	--	--
311-9	2000	S	3.54	28.0	2.10	57.0
311-19	700	S	3.63	18.0	--	--
311-20	2000	S	3.53	27.2	2.10	46.0
311-21	2000	S	3.52	27.2	2.10	54.0
311-22	2000	2P	2.49 3.45	29.0	2.12	>125.0
311-25	700	S	3.70	21.0	--	--
311-30A	2000	S	3.51	23.4	2.10	54.0
311-31	2000	S	3.50	25.0	2.10	51.0
312-8	2000	S	3.52	27.0	2.10	42.0
312-9	2000	2P	3.52 3.45	27.0	2.10	57.0
312-10	700	S	3.65	16.2	--	--
312-10	2000	S	3.49	35.0	2.11	53.0
312-14	2000	S	3.51	29.0	2.09	61.0
312-14A	2000	3P	3.46 3.43 3.36	32.0	2.12	>150.0
312-15	2000	S	3.52	27.1	2.11	51.0
312-16	2000	3P	3.47 3.43 3.36	32.1	2.11	51.0
312-21	2000	S	3.51	30.8	2.10	57.0
312-26	2000	S	3.51	27.8	2.09	48.0
312-28	2000	S	3.51	27.2	2.10	51.0
312-29	2000	S	3.51	34.0	2.10	57.0
312-31, solid	2000	S	3.57	27.6	2.10	56.0
312-32	2000	S	3.51	30.8	2.10	54.0
312-33	2000	NVS	3.48	30.8	2.10	52.8

Sample Designation	Temp. (°C)	(002) Peak Type	d(002)	Lc	d(10)	La
312-34	2000	2P	3.46 3.44	33.0	2.11	46.2
312-39	2000	S	3.49	29.8	2.10	53.0
312-40	2000	2P	3.48 3.45	30.1	2.09	54.0
312-43	2000	2P	3.48 3.43	33.2	2.11	51.0
312-44	2000	2P	3.48 3.44	42.0	2.11	51.0
312-48	2000	3P	3.46 3.43 3.37	30.4	2.10	37.0
312-49	2000	S	3.52	31.1	2.11	61.0
315-1	2000	S	3.53	27.2	2.10	48.0
315-2	2000	2P	3.49 3.43	29.0	2.10	54.0
315-3	700	S	3.71	16.2	--	--
315-5	2000	2P	3.49 3.44	29.0	2.11	54.0
315-8	2000	2P	3.49 3.44	28.2	2.10	56.0
315-9	2000	2P	3.47 3.44	33.0	2.11	47.0
315-14	2000	S	3.53	26.3	2.10	54.0
315-18	2000	3P	3.40 3.382 3.351	45.0	--	--
315-20	680	S	3.70	16.3	--	--
315-20A	2000	2P	3.53 3.43	28.0	2.10	57.0
315-21C	2000	2P	3.52 3.43	27.8	2.10	57.0
315-22	665	S	3.67	16.4	--	--
315-22	2000	S	3.52	28.0	2.10	51.0
315-24A	2000	2P	3.47 3.38	20.0	--	--
315-25A	2000	S	3.52	26.5	2.09	48.0
315-26B	2000	3P	3.50 3.41 3.37	26.5	2.10	46.0
315-26C	680	S	3.69	17.1	--	--
315-28	2000	2P	3.52 3.43	26.0	2.10	46.0
315-28B	600	S	3.70	16.8	--	--
315-30	2000	2P	3.56 3.43	24.0	2.09	48.0
315-31	680	S	3.70	18.2	--	--
315-34	680	S	3.69	15.4	--	--

Sample Designation	Temp. (°C)	(002) Peak Type	d(002)	Lc	d(10)	La
315-36	2000	3P	3.52	24.3	2.10	48.5
			3.43			
			3.37			
315-37	680	S	3.63	17.5	--	--
315-37	2000	S	3.50	26.3	2.098	42.0
315-38	680	S	3.63	18.8	--	--
315-38	2000	2P	3.49	27.1	2.097	46.0
			3.43			
315-39	2000	2P	3.53	27.2	2.098	57.0
			3.43			
315-39	680	S	3.63	20.0	--	--
315-40	2000	S	3.54	25.6	2.097	51.0
315-41	2000	NVS	3.49	23.6	2.098	51.0
315-42	2000	S	3.56	27.2	2.098	46.0
315-43	2000	NVS	3.52	24.3	2.098	51.0
315-43	700	S	3.67	17.4	--	--
315-44	2000	2P	3.55	23.1	2.10	40.2
			3.45			
315-45	2000	S	3.49	27.2	2.10	46.6
315-46A	2000	2P	3.55	23.1	2.098	57.0
			3.43			
316-6	2000	NVS	3.50	27.0	2.11	57.0
316-7, Run 1	2000	S	3.49	28.0	2.10	45.0
316-7, Run 2	2000	S	3.52	27.0	2.10	53.0
316-15	2000	2P	3.40	32.0	--	--
316-28	2000	S	3.50	27.2	2.10	51.0
316-32	2000	2P	3.42	53.0	--	--
			3.40			
317-1	700	S	3.71	20.0	--	--
317-1	2000	S	3.46	45.0	2.11	63.0
317-2	700	S	3.68	15.7	--	--
317-2	2000	NVS	3.48	24.6	2.09	47.0
317-6	700	S	3.71	13.0	--	--
317-6	2000	NVS	3.55	22.0	2.10	55.0
317-7	700	S	3.68	16.0	--	--
317-7	2000	NVS	3.46	27.5	2.10	50.0
317-8	700	S	3.71	11.5	--	--
317-8	2000	2P	3.56	20.0	2.10	44.0
			3.46			
317-10	2000	NVS	3.48	26.0	2.10	68.0
317-11	700	S	3.71	16.3	--	--
317-13	700	S	3.72	15.0	--	--
317-13	2000	NVS	3.47	24.0	2.08	66.0
317-14	700	S	3.71	15.7	--	--
317-14	2000	NVS	3.45	27.0	2.09	46.0
317-15	700	S	3.71	15.3	--	--
317-15	2000	NVS	3.47	26.0	2.09	54.0
317-16	2000	S	3.54	24.0	2.09	53.0

Sample Designation	Temp. (°C)	(002) Peak Type	d(002)	Lc	d(10)	La
317-18	2000	S	3.59	21.0	2.09	58.0
317-19	700	S	3.68	16.5	--	--
317-19	2000	NVS	3.49	30.0	2.09	52.0
317-20	700	S	3.66	17.5	--	--
317-20	2000	S	3.50	25.6	2.09	48.0
317-24, Run 1	2000	NVS	3.52	24.0	2.09	45.0
317-24, Run 2, solid	2000	NVS	3.49	21.0	2.09	50.0
317-25	2000	S	3.53	20.0	2.09	50.0
317-26, Run 1	2000	NVS	3.48	26.0	2.09	48.0
317-26, Run 2, solid	2000	2P	3.46 3.43	24.2	2.10	51.0
317-28	2000	NVS	3.46	25.0	2.09	52.0
317-29	700	2P	3.43 3.42	21.5	--	--
317-29, Run 1	2000	NVS	3.43	65.0	--	--
317-29, Run 2	2000	NVS	3.426	75.0	--	--
317-30	2000	2P	3.44 3.40	29.5	--	--
317-31A	2000	S	3.58	22.0	2.10	46.0
317-32	700	S	--	--	--	--
317-32	2000	2P	3.51 3.48	23.6	2.08	49.0
317-33	700	S	3.68	17.0	--	--
317-33	2000	S	3.414	92.0	2.10	49.0
317-34	700	S	3.68	17.0	--	--
317-34	2000	3P	3.44 3.42 3.36	30.0	2.09	50.0
317-35	700	S	3.71	16.0	--	--
317-35	2000	3P	3.50 3.43 3.36	26.5	2.10	62.0
317-37	700	S	3.68	15.6	--	--
317-37	2000	NVS	3.43	43.0	2.10	63.0
317-38	700	S	3.68	15.6	--	--
317-38	2000	3P	3.54 3.43 3.37	25.0	2.09	51.0
317-39, Run 1	2000	3P	3.45 3.43 3.36	28.0	2.10	52.0
317-39, Run 2, solid, 1mm thick	2000	3P	3.52 3.42 3.37	24.2	2.09	45.0
317-39, Run 3, solid, 1mm thick	2000	3P	3.52 3.41 3.37	23.5	2.09	49.0

Sample Designation	Temp. (°C)	(002) Peak Type	d(002)	Lc	d(10)	La
317-40	2000	3P	3.49	24.8	2.10	48.0
			3.42			
			3.36			
317-41A	2000	S	3.53	26.5	2.10	48.0
317-41B	2000	S	3.53	28.0	2.10	54.0
317-42	2000	3P	3.49	26.0	2.10	42.6
			3.42			
			3.36			
317-43	2000	3P	3.45	26.0	2.09	56.0
			3.42			
			3.35			
317-44	2000	3P	3.48	30.0	2.09	55.0
			3.42			
			3.36			
317-45, solid, 1mm thick	700	S	3.75	12.9	--	--
317-45, Run 1	2000	3P	3.48	25.0	2.09	60.0
			3.40			
			3.35			
317-45, Run 2	2000	3P	3.46	24.0	2.09	42.0
			3.42			
			3.35			
317-46	2000	3P	3.43	31.5	2.10	75.0
			3.42			
			3.36			
317-47	2000	3P	3.50	27.0	2.10	60.0
			3.42			
			3.36			
317-48, Run 1	700	S	3.71	16.2	--	--
317-48, Run 2	700	S	3.87	17.4	--	--
317-48, Run 1	2000	3P	3.45	40.0	2.10	60.0
			3.43			
			3.37			
317-48, Run 2 solid, 1mm thick	2000	3P	3.46	34.0	2.10	59.0
			3.43			
			3.37			
317-49	700	S	3.71	15.7	--	--
317-49, Run 1	2000	3P	3.49	29.0	2.09	62.0
			3.41			
			3.35			
317-49, Run 2 solid, 1mm thick	2000	3P	3.46	33.0	2.09	60.0
			3.44			
			3.37			
317-50	700	S	3.67	15.6	--	--
318-1	2000	S	3.55	28.0	2.10	54.0
318-2	2000	S	3.51	27.0	2.10	55.0
318-3, Run 1	700	S	3.70	16.7	--	--
318-3, Run 2	700	S	3.69	16.7	--	--

Sample Designation	Temp. (°C)	(002) Peak Type	d(002)	Lc	d(10)	La
318-3	2000	2P	3.46 3.41	26.0	2.11	51.0
318-4	700	S	3.66	16.8	--	--
318-6A	2000	S	3.50	31.0	2.09	59.0
318-7, Run 1	2000	S	3.50	28.0	2.10	65.0
318-7, Run 2, solid	2000	S	3.49	28.0	2.10	45.0
318-8, Run 1	2000	S	3.45	39.0	2.10	63.0
318-8, Run 2 solid, 2mm thick	2000	S	3.45	43.5	2.10	77.0
318-9	2000	2P	3.48 3.46	32.5	2.11	57.0
318-10	520	S	3.74	15.2	--	--
318-10	2000	S	3.49	33.8	2.12	50.0
318-11, Run 1	2000	NVS	3.42	77.0	2.10	38.0
318-11, Run 2	2000	NVS	3.43	78.0	2.11	40.0
318-12	2000	3P	3.49 3.43 3.36	31.4	2.09	59.0
318-13	2000	NVS	3.42	44.0	2.10	58.0
318-14	700	S	3.65	16.0	--	--
318-14	2000	3P	3.48 3.43 3.36	30.5	2.10	60.0
318-15, Run 1	700	S	3.75	16.0	--	--
318-15, Run 2	700	S	3.75	15.1	--	--
318-15	2000	3P	3.45 3.42 3.37	30.2	2.10	60.0
318-16	700	S	3.72	15.7	--	--
318-16	2000	2P	3.43 3.41	39.0	2.09	49.0
318-17	700	S	3.68	16.7	--	--
318-17	2000	NVS	3.45	42.0	2.11	59.0
318-18, Run 1	700	S	3.68	16.4	--	--
318-18, Run 2	700	S	3.71	16.3	--	--
318-18	2000	S	3.55	25.6	2.10	44.0
318-19	2000	S	3.52	26.0	2.09	59.0
318-20	700	S	3.67	16.0	--	--
318-20	2000	S	3.53	21.0	2.09	48.0
318-21, Run 1	700	S	3.78	14.0	--	--
318-21, Run 2	700	S	3.75	15.4	--	--
318-21	2000	S	3.55	23.6	2.10	55.0
318-22	700	S	3.70	15.4	--	--
318-22, Run 1	2000	NVS	3.44	65.0	2.10	55.0
318-22, Run 2	2000	NVS	3.44	64.0	2.11	54.0
318-23	700	S	3.74	16.0	--	--
318-23	2000	S	3.63	63.0	2.10	73.0
318-24	700	S	3.64	16.7	--	--

Sample Designation	Temp. (°C)	(002) Peak Type	d(002)	Lc	d(10)	La
318-24	2000	S	3.44	45.0	2.10	68.0
318-26, Run 1	700	S	3.69	15.7	--	--
318-26, Run 2	700	S	3.75	16.1	--	--
318-26, Run 3	700	S	3.69	16.7	--	--
318-27	2000	2P	3.45 3.41	35.4	2.10	47.0
318-28	700	S	3.75	18.0	--	--
318-28	2000	2P	3.47 3.42	27.0	--	--
318-29, Run 1	2000	NVS	3.45	30.0	2.08	62.0
318-29, Run 2, solid, 1mm thick	2000	2P	3.50 3.44	30.5	2.10	65.0
318-29, Run 3	2000	2P	3.52 3.42	31.0	2.10	60.0
318-30	700	S	3.64	15.2	--	--
318-30, Run 1	2000	2P	3.48 3.43	34.1	2.11	69.0
318-30, Run 2	2000	3P	3.45 3.41 3.36	31.0	2.11	63.0
318-31, Run 1	2000	2P	3.45 3.43	35.5	2.10	64.0
318-31, Run 2	2000	3P	3.47 3.41 3.36	31.0	2.11	63.0
318-32, Run 1	700	S	3.64	15.7	--	--
318-32, Run 2	700	S	3.63	16.0	--	--
318-32	2000	S	3.44	47.0	2.10	65.0
318-33	700	S	3.66	16.7	--	--
318-33	2000	NVS	3.46	28.0	2.11	64.0
318-34	700	S	3.63	16.5	--	--
318-34	2000	3P	3.49 3.43 3.36	37.0	2.10	59.0
318-35	700	S	3.71	15.3	--	--
318-35	2000	3P	3.50 3.44 3.37	34.0	2.11	67.0
318-36	700	S	3.68	17.0	--	--
318-36	2000	2P	3.51 3.44	28.0	2.10	49.0
318-37	700	S	3.71	16.1	--	--
318-37	2000	3P	3.46 3.43 3.376	33.6	2.10	52.0
318-38	700	S	3.71	15.6	--	--
318-38	2000	3P	3.47 3.43 3.37	28.0	2.10	49.0

Sample Designation	Temp. (°C)	(002) Peak Type	d(002)	Lc	d(10)	La
318-39, Run 1	700	S	3.71	17.0	--	--
318-39, Run 2 solid, 1mm thick	700	S	3.65	17.2	--	--
318-39	2000	S	3.51	26.1	2.09	60.0
318-40	700	S	3.71	15.0	--	--
318-40	2000	2P	3.52 3.45	28.0	2.11	54.0
318-41	700	S	3.71	14.8	--	--
318-41	2000	S	3.50	28.0	2.09	57.0
318-43, Run 1	700	S	3.69	17.0	--	--
318-43, Run 2 solid, 1mm thick	700	S	3.71	13.8	--	--
318-43, solid	2000	S	3.44	31.0	2.12	58.0
318-44	700	S	3.72	15.6	--	--
318-44	2000	S	3.55	27.2	2.10	44.0
318-45	700	S	3.71	15.7	--	--
318-45	2000	S	3.56	25.4	2.10	46.0
318-46	700	S	3.71	15.9	--	--
318-46, solid 1mm thick	2000	S	3.53	26.2	2.11	51.0
318-47	700	S	3.71	15.0	--	--
318-47	2000	NVS	3.49	29.0	2.10	48.0
318-48, Run 1	2000	S	3.53	26.8	2.10	54.0
318-48, Run 2	2000	S	3.52	29.2	2.10	42.0
318-50, Run 1	700	S	3.71	14.3	--	--
318-50, Run 2	700	S	3.71	15.5	--	--
318-50	2000	S	3.53	26.0	2.10	46.0
318-51	2000	S	3.56	27.2	2.10	56.0
318-52	2000	S	3.53	26.5	2.10	54.0
318-53, Run 1	2000	S	3.52	26.5	2.10	54.0
318-53, Run 2	2000	S	3.54	30.0	2.10	60.0
318-54	700	S	3.66	17.0	--	--
318-55	700	S	3.71	15.2	--	--
318-56	2000	S	3.54	27.0	2.10	54.0
318-58	700	S	3.71	18.0	--	--
318-58	2000	NVS	3.51	28.2	2.10	51.0
318-59	700	S	3.68	16.7	--	--
318-59	2000	S	3.51	26.0	--	--
318-60	700	S	3.70	15.7	--	--
318-60	2000	2P	3.47 3.44	32.0	--	--
318-61	700	S	3.71	18.6	--	--
318-61	2000	S	3.52	23.3	2.09	55.0
318-62	700	S	3.70	15.3	--	--
318-62	2000	S	3.56	22.5	2.10	51.0
321-1	700	S	3.66	5.0	--	--
321-2	700	2P	3.63 3.57	17.4	--	--

Sample Designation	Temp. (°C)	(002) Peak Type	d(002)	Lc	d(10)	La
321-2	2000	3P	3.54	22.8	2.10	51.5
			3.43			
			3.38			
321-3	700	S	3.64	17.4	--	--
321-3	2000	S	3.53	24.3	2.10	51.0
321-4	700	S	3.64	17.2	--	--
321-4	2000	-	--	--	--	--
321-5	700	S	3.63	15.4	--	--
321-5	2000	S	3.49	26.4	2.09	53.7
321-6	700	S	3.64	17.0	--	--
321-6	2000	S	3.54	27.7	2.10	48.0
321-7	700	S	3.69	18.0	--	--
321-7	2000	-	--	--	--	--
321-8	700	S	3.69	17.5	--	--
321-8	2000	-	--	--	--	--
321-9	700	S	3.67	17.4	--	--
321-9	2000	-	--	--	--	--
321-10	700	S	3.67	17.0	--	--
321-10	2000	-	--	--	--	--
321-11	700	S	3.71	17.0	--	--
321-11	2000	2P	3.54	27.2	2.10	65.0
			3.46			
321-12	700	S	3.63	16.8	--	--
321-12	2000	S	3.53	26.4	2.094	56.0
321-13	700	S	3.66	17.0	--	--
321-16A	2000	3P	3.50	30.8	2.10	57.0
			3.43			
			3.36			
321-16B	2000	S	3.50	28.8	2.10	44.0
321-16C	700	S	3.63	15.2	--	--
321-17	700	S	3.60	18.7	--	--
321-17B	2000	S	3.49	28.8	2.10	44.0
321-18A	2000	3P	3.50	29.8	2.10	49.0
			3.43			
			3.37			
321-18B	700	S	3.63	15.2	--	--
321-19A	2000	2P	3.54	25.0	2.09	46.0
			3.426			
321-19A	700	S	3.63	17.1	--	--
321-19B	2000	NVS	3.43	39.0	2.10	53.8
321-20A	700	S	3.63	17.5	--	--
321-20A	2000	3P	3.52	28.0	2.10	61.0
			3.42			
			3.36			
321-20B	2000	3P	3.53	37.0	2.10	46.0
			3.426			
			3.37			
321-21A	700	S	3.63	18.0	--	--

Sample Designation	Temp. (°C)	(002) Peak Type	d(002)	Lc	d(10)	La
321-21A	2000	NVS	3.43	41.6	2.10	51.0
321-21B	700	S	3.64	18.4	--	--
321-21B	2000	S	3.52	27.0	2.10	57.0
321-22A	2000	2P	3.52	27.6	2.10	53.0
			3.43			
321-22B	700	S	3.70	16.1	--	--
321-23	2000	S	3.49	33.0	2.10	54.0
321-23A	700	S	3.63	18.4	--	--
321-23B	700	S	3.36	16.5	--	--
321-23B	2000	3P	3.52	29.6	2.10	51.0
			3.43			
			3.36			
321-24	700	S	3.70	15.8	--	--
321-24A	700	S	3.63	16.2	--	--
321-24B	700	S	3.63	16.5	--	--
321-24B	2000	S	3.43	35.4	2.09	57.0
321-25	700	S	3.63	18.4	--	--
321-25	2000	NVS	3.47	30.8	2.10	60.8
321-25A	700	S	3.60	21.0	--	--
321-25A	2000	NVS	3.43	40.2	2.10	60.5
321-26	700	S	3.67	15.0	--	--
321-26	2000	S	3.52	27.2	2.094	48.5
321-26A	700	S	3.63	18.1	--	--
321-26A	2000	S	3.52	27.2	2.094	54.0
321-27	2000	S	3.52	29.8	2.10	51.0
321-29	700	S	3.63	16.8	--	--
321-29	2000	3P	3.49	24.8	2.094	58.0
			3.40			
			3.35			
321-30	700	S	3.63	19.6	--	--
321-31	2300	3P	3.44	49.0	2.10	60.5
			3.41			
			3.37			
321-31A	2300	NVS	3.40	90.0	2.11	58.0
321-31B	2300	3P	3.49	37.0	2.11	69.0
			3.43			
			3.37			
321-31C	700	S	3.60	18.8	--	--
321-31C	2300	3P	3.49	34.5	2.11	69.0
			3.426			
			3.37			
321-31D	700	S	3.63	17.4	--	--
321-31D	2300	S	3.47	37.2	2.11	69.0
321-31E	700	S	3.63	17.4	--	--
321-31E	2300	NVS	3.426	61.6	2.11	69.0
321-31F	700	S	3.60	18.5	--	--
321-31F	2300	S	3.45	44.0	2.10	69.0
321-31G	2300	2P	3.47	35.0	2.10	56.0
			3.43			

Sample Designation	Temp. (°C)	(002) Peak Type	d(002)	Lc	d(10)	La
321-31I	2300	2P	3.49 3.38	40.0	2.11	69.0
321-32	700	S	3.60	18.9	--	--
321-34A	2300	S	3.426	51.4	2.10	42.0
321-36A	2300	S	3.47	53.6	2.11	64.5
321-36B	700	S	3.63	18.2	--	--
321-36C	2300	S	3.43	70.0	2.10	46.0
321-37	2000	S	3.52	30.8	2.10	54.0
321-37A	700	S	3.60	18.1	--	--
321-37B	2000	3P	3.53 3.44 3.36	27.2	2.10	54.0
321-38B	700	S	3.63	17.7	--	--
321-39	2000	2P	3.48 3.426	34.1	2.10	57.0
321-39B	700	S	3.63	16.4	--	--
321-41C	2000	3P	3.49 3.43 3.36	32.6	2.10	62.5
321-42A	700	S	3.63	18.8	--	--
321-42A	2000	2P	3.49 3.43	35.5	2.10	60.5
321-42B	700	S	3.63	16.7	--	--
321-42B	2000	2P	3.50 3.43	25.3	2.10	64.4
321-43B	700	S	3.63	19.3	--	--
321-43B	2000	2P	3.49 3.42	35.0	2.098	59.4
321-43B$_1$	2000	2P	3.50 3.426	36.8	2.11	59.5
321-43B$_2$	2000	2P	3.50 3.43	33.0	2.10	57.0
321-44A	2000	3P	3.50 3.43 3.36	30.8	2.10	51.0
321-44B	2000	3P	3.50 3.43 3.36	29.0	2.10	54.0
321-45A	2200	S	3.49	33.0	2.10	57.0
321-45B	2200	S	3.47	45.5	2.10	40.5
321-46A	2000	2P	3.49 3.43	31.7	2.10	60.4
321-46B	2000	3P	3.46 3.43 3.36	30.8	2.10	51.0
321-46C	2000	3P	3.47 3.43 3.36	35.6	2.10	51.0

Sample Designation	Temp. (°C)	(002) Peak Type	d(002)	Lc	d(10)	La
321-46D	2000	3P	3.50	31.7	2.10	64.4
			3.43			
			3.36			
321-48A	2000	S	3.50	31.8	2.10	57.0
321-48B	2000	S	3.50	33.0	2.10	64.4
321-48C	2000	S	3.50	33.0	2.10	60.4
321-49A	2000	S	3.49	33.0	2.10	60.4
321-49B	2000	NVS	3.426	51.2	2.10	54.0
321-51	2000	NVS	3.43	91.5	2.11	69.0
321-51A	2000	NVS	3.43	107.5	2.11	68.0
321-52	2000	NVS	3.43	91.2	2.11	60.5
322-1A	2000	3P	3.44	26.4	2.085	57.3
			3.37			
			3.33			
322-1B	2000	S	3.40	41.5	2.085	--
322-2B	1600	S	3.50	23.0	2.085	37.3
322-3B	1600	S	3.53	22.0	2.085	61.0
322-10A	2000	2P	3.46	33.0	2.085	--
			3.42			
322-10B	2000	2P	3.50	30.8	2.10	69.0
			3.43			
322-10C	2000	2P	3.49	33.4	2.085	--
			3.43			
322-10D	2000	2P	3.50	28.6	2.10	60.0
			3.43			
322-11A	1670	S	3.55	22.0	2.085	51.2
322-12A	1600	S	3.56	23.0	2.085	40.5
322-12B	1670	S	3.56	22.0	2.10	57.0
322-13B	1670	S	3.53	31.8	2.085	50.2
322-14A	1670	S	3.50	23.0	2.085	--
322-14B	1670	S	3.56	21.0	2.09	46.0
322-15B	1670	S	3.56	25.0	2.085	48.4
322-16A	1670	S	3.56	23.5	2.085	--
322-16B	1670	S	3.56	22.0	2.085	44.0
322-17A	1670	S	3.56	22.2	2.085	88.0
322-17B	1670	S	3.56	22.0	2.085	51.4
322-18B	1670	S	3.50	28.8	2.085	61.5
322-19B	1670	S	3.56	20.6	2.085	48.5
322-20	1670	S	3.50	21.4	2.085	30.2
322-21B	1670	S	3.56	17.0	2.085	69.5
322-25A	1410	S	3.56	18.5	2.085	46.1
322-25B	1410	S	3.56	19.2	2.07	121.0
322-26A	1410	S	3.50	25.6	2.085	51.0
322-26B	1410	S	3.50	19.2	2.085	40.2
322-27A	1410	S	3.59	20.0	2.085	57.3
322-27B	1410	S	3.56	19.3	2.085	--
322-28A	1410	S	3.56	19.4	2.08	42.0
322-28B	1410	S	3.56	17.8	2.085	53.2

Sample Designation	Temp. (°C)	(002) Peak Type	d(002)	Lc	d(10)	La
322-29	1410	S	3.56	20.1	2.085	40.2
322-29B	1410	S	3.56	21.0	2.085	53.2
322-31A	1410	S	3.56	23.0	2.085	40.4
322-36	1543	S	3.56	19.2	2.085	53.0
322-37	1543	S	3.56	23.0	2.085	--
322-40	1440	S	3.53	23.6	2.085	66.0
322-41	1440	S	3.56	20.4	2.085	61.0
322-42A	1440	S	3.56	21.4	2.085	37.1
322-42B	1440	S	3.56	21.4	2.085	65.0
322-46	1440	S	3.53	19.6	2.08	--
322-47A	1440	S	3.50	21.5	2.085	74.0

TABLE 2   Sizes of the Structural Features Observed in Bright and Dark Field Electron Micrographs Compared to Crystallite Sizes Obtained from X-ray Analysis

Sample #	Platelet Dia. Å	Granu-lation* Dia. Å	Dark Field Dia. Å** (002)	(100)	X-ray (Å) Lc	La	(002) Peak Type
311-19(2000)	150-500	30-40	20-40	--	--	--	--
311-19(750)×	150-350	20-30	--	--	14	19	S
312-31(2000)	200-500	20-45	20-45	--	27.6	56	S
312-31(2000)	150	35	30	>100	28	56	S
317-24(2000)	250	42	60†	--	24	45	NVS
317-29(2000)	>250	60	30-70†	--	65-75	--	NVS
317-33(2000)	250-500	35	--	--	92	49	S
317-45(2000)	>500	30	--	--	25	60	3P
317-48(2000)×	250	55	--	--	34	59	3P
317-49(2000)×	250-500	45	40†	--	33	60	3P
318-12(2000)	250-500	60	50	110†	31	59	3P
318-22(2000)	>500	40-60	35	--	65	55	NVS
318-22(700)	250	--	--	--	15.7	--	S
318-23(2000)	250	50	50	--	63	73	S
318-23(700)	--	--	--	--	16	--	S
318-29(2000)×	>500	30-40	60	--	31	63	2P
321-31C(2000)×	250	35	60	80	35	69	3P
321-31D(2300)	250	40	35	80	37	69	S

*Diameter corresponds to distances between nearest neighbor.
**Diameter of diffracting regions obtained from (002) or (100) diffraction halos.
†Some of the crystallites giving rise to halos or spots are very large in size, i.e., up to 500Å.
×A second structural feature was observed in the bright field micrographs of these samples. This new feature appeared to be long regular cylinders 500Å in diameter by about 1μ long. Regular striations along the length were spaced 45Å apart.

TABLE 3 — Electron Diffraction Results Compared to X-ray Diffraction Results for d(002) and d(10) Spacings (Å)

Sample #	X-ray d(002)	X-ray d(10)	Electron Diffraction d(002)	Electron Diffraction d(10)	(002) Peak Type
Graphite	3.35	2.13	3.37	3.12	--
311-19(2000)	3.56	2.17	3.45	2.09	--
311-19(750)	3.70	2.19	--	2.07	S
312-31(2000)	3.54	2.12	3.53	2.16	S
	3.57	2.10	3.53†	2.12	S
317-24(2000)	3.50	2.10	3.53†	2.10†	NVS
317-29(2000)	3.43	--	3.35†	2.12	NVS
			3.45		
317-33(2000)	3.414	2.10	3.35†	2.10	S
317-45(2000)	3.35	2.09	3.50	2.10	3P
	3.48				
317-48(2000)	3.46	2.10	3.48†	2.12	3P
317-49(2000)	3.48	2.09	3.48†	2.10	3P
318-12(2000)	3.49	2.09	3.47†	2.11	3P
318-22(2000)	3.44	2.10	3.37†	2.07	NVS
318-22(700)	3.70	--	3.50	2.11	S
			3.42†		
318-23(2000)	3.43	2.10	3.50†	2.10	S
318-23(700)	3.74	--	--	2.07	S
318-29(2000)	3.45	2.08	3.45	2.12	2P
321-31C(2300)	3.43	2.11	3.56†	2.12	3P
321-31D(2300)	3.47	2.11	3.50*	2.125	S

*In this sample no spots were seen on any diffraction halo.
†In addition to Debye-Scherrer rings, a number of sharp diffracting spots were observed on or close to the ring.

TABLE 4

Sample	a in Å		Dispersity
	Our value	Reported Value	
LMSC-20	42.4	17.1	Monodisperse
GC-10	14.0	9.0	"
GC-20	12.9	11.5	"

TABLE 5

Sample	a in A	Dispersity
312-31 (2000)	40.8	Polydisperse
317-45 (2000)	21.2	Wide distribution of pores
318-11 (2000)	20.4 ⎫ 44.4 ⎭	Bidisperse
318-41B (700)	18.7	Monodisperse
318-42 (2000)	41.0	Polydisperse
318-44 (2000)	30.4	Monodisperse
318-45 (700)	28.0	Monodisperse
318-45 (2000)	35.3	Monodisperse
318-46 (2000)	20.4	Monodisperse
318-48 (700)	9.5	Monodisperse
318-48 (2000)	25.4	Monodisperse

TABLE 6

Sample #	Temp.°C	He Density (gm/cm^3)	Surface Area Knudsen Flow (m^2/gm)	Specific Surface Area (m^2/gm)
311-32	2000	1.41	3.0	26.4
317-9	700	1.83	--	506.0
317-9	2000	1.70	12.5	59.9
317-12	700	1.80	9.1	510.0
317-12	2000	1.72	--	109.0
318-22	700	1.79	--	459.0
318-22	2000	1.51	--	49.6
321-9	700	1.46	--	541.2
321-9	2000	1.36	--	12.7

TABLE 7

Sample #	Temp.°C	$\rho_{He\ real}$[1] (g/cc)	$\rho_{Hg\ real}$[2] (g/cc)	$\rho_{Hg\ app.}$ (g/cc)	MPD (μ)	IPV (cc/g)
GC No.1		1.47	1.482	1.424	.003	.0273
302-5	2320	--	1.509	.647	2.97	.8828
302-12	2320	--	1.501	.559	3.62	1.1224
305-6	2000	1.94	1.802	.636	2.54	1.0151
6.62 Mo						
305-12	2000	1.55	1.562	.557	4.19	1.1560
305-18	2000	1.77	1.718	.606	2.49	1.0678
.4 Mo						
308P-2 #2		1.586	1.505	1.034	.009	.3030
308P-3 #3		1.611	1.486	1.077	.008	.2559
310-1	1000	1.27	1.446	.814	.023	.5411
310-3	1000	--	1.424	.805	.020	.5454
310-17A	2000	1.50	1.175	.639	.119	.7130
310-18	1000	1.48	1.452	.687	.039	.7666
310-18	2000	1.15	1.366	.648	.044	.8110
310-20	2000	1.09	1.458	1.029	.009	.2855
310-29	2000	1.89	1.533	.944	.014	.3959
311-21	2000	1.59	1.339	.731	.038	.6221
311-22	2000	1.00	.847	.484	.154	.8809
312-19A	730	1.20	1.481	.879	.629	.4626
312-29	728	1.52	1.441	1.038	.014	.2709
312-31	2000	1.41	1.490	.923	.025	.4118
312-45	2000	1.26	1.302	1.214	.005	.0540
312-48	2000	1.53	1.392	.861	.121	.4425
312-49	2000	1.34	1.404	1.031	.011	.2579
315-1	2000	1.50	1.431	.962	47.0	.3412
317-5	2000	1.42	1.313	.873	.071	.4039
317-18	2000	1.50	1.255	.953	39.1	.281
318-22	700	1.79	1.426	.771	.057	.5958
318-22	2000	1.51	1.576	.937	.054	.4334
318-45	2000	--	1.20	.78	.0078	.021
321-9	700	1.46	1.24	.98	.0073	.205
321-9	2000	1.26	1.4	1.2	.0057	.016
321-17	2000	1.43	1.17	.59	2.15	.299
321-18	2000	1.67	1.16	.87	.175	.247
321-19	2000	1.80	1.56	.98	.049	.379
321-20	2000	1.60	1.63	.70	.088	.345
321-21	2000	1.79	1.30	.85	.041	.377
321-25	2000	--	2.20	1.14	.011	.088

---

*Glassy Carbon No. 1 - Le Carbone, p. 6927.
[1]Real density as determined by He pycnometry
[2]Real density as determined by Hg

Sample #	Temp.°C	ρ_{He} real[1] (g/cc)	ρ_{Hg} real[2] (g/cc)	ρ_{Hg} app. (g/cc)	MPD (μ)	IPV (cc/g)
321-31	2000	1.41	1.49	1.34	.0195	.075
322-14A	1300				2.2	.826
322-14A	1412	1.74			1.7	.494
322-14B	1300				2.3	.501
322-14B	1412				1.5	.496
322-17A	1300				4.5	.604
322-17A	1412				4.4	.271
322-17B	1300				2.5	.382
322-17B	1412				2.0	.534
322-19A	1300				1.0	.461
322-19A	1412	1.9			.08	.472
322-19B	1300				.65	.466
322-19B	1412				.95	.468
322-20	1300				1.8	.432
322-20	1412				1.5	.666
322-21A	1300				18.	.503
322-21A	1412				3.5	.420
322-21B	1412				10.	.400
322-21D	1300				8.	.780
322-22A	1300				1.1	.308
322-22A	1412				1.2	.443
322-22B	1300				1.4	.457
322-22B	1412	1.49X*			1.2	.440
322-23A	1300				1.5	.443
322-23A	1412				1.2	.458
322-23B	1300	2.03X			.32	.453
322-23B	1412				.35	.458
322-24A	1300	1.74X			1.3	.395
322-24A	1412				1.3	.563
322-24B	1300				1.9	.620
322-24B	1412	1.59X			1.4	.888
322-32	1350	1.60X			1.4	.571
322-35	1350	1.43X			6.0	.472
322-41	1440	1.59X			.07	.669
322-45	1500	1.72X			4.2	.421
322-46	1500				1.4	.550
322-47A	1500				1.3	.652
322-48	1605				6.0	.634
322-49	1400				7.0	.841
322-49	1400				7.0	.607
322-49	1600				7.0	.595
322-50	1600				6.0	.545
322-50	1400				6.0	.679

*X indicates Xylene

TABLE 8

Physical Properties

Sample #	Temp.°C	$\rho_{app.}$ (g/cc)	ρ_{He} (g/cc)	Resistivity Ω-cm(×10)	Hardness (DPH)	Int. Frict. (×10³)	Sonic Mod. psi (×10⁻⁶)	Compr. str. psi (×10⁻³)	Ult. Str. psi (×10⁻³)
310-35	2000	0.57	--	--	--	--	--	5.18	1.01
311-34	2000	0.60	--	--	--	--	--	7.2	7.04
311-35	2000	0.51	--	.294	--	1.43	0.35	6.85	1.23
312-13	2000	1.07	--	--	--	--	--	50.0	4.85
312-14	2000	1.00	1.44	--	--	--	--	36.0	--
312-16	2000	0.77	1.27	--	--	--	--	1.73	2.83
312-27	2000	1.15	--	--	--	--	--	--	7.78
312-29	2000	1.07	1.52	--	--	--	--	39.7	--
312-32	2000	0.90	1.47	--	--	--	--	29.2	5.13
312-33	2000	--	1.59	--	90	--	--	--	--
312-34	2000	0.92	1.38	--	--	--	--	27.3	1.11
312-44	2000	--	1.18	--	98	--	--	--	--
312-45	680	--	--	--	135	--	--	--	--
321-45A	2000	--	1.26	--	176	--	--	--	--
312-46	680	--	--	--	107	--	--	--	--
312-46	2000	--	--	--	165	--	--	--	--
312-49	2000	1.10	1.3	--	--	--	--	--	5.96
315-1	2000	0.89	1.49	--	--	--	--	--	--
315-2	2000	0.70	1.52	.349	--	--	1.27	1.47	0.36
315-3	2000	--	1.38	--	--	--	--	--	--
315-4	2000	--	1.55	--	--	--	--	--	--
315-14	2000	0.96	1.6	--	--	--	--	47.7	4.7
315-17	2000	0.79	--	--	--	--	--	29.3	2.51
315-20	2000	0.84	1.6	--	--	--	--	--	--
315-20A	2000	0.84	1.6	.180	--	0.93	1.48	--	--
315-20B	2000	0.77	1.60	.275	--	1.63	1.37	--	--
315-20C	2000	0.88	1.60	.203	--	0.54	1.52	--	--
315-21B	2000	0.96	--	--	--	--	--	--	6.60
315-21C	2000	0.91	1.52	.147	--	0.26	1.54	46.8	7.13

Sample #	Temp.°C	$\rho_{app.}$ (g/cc)	ρ_{He} (g/cc)	Resistivity Ω-cm(×10)	Hardness (DPH)	Int. Frict. (×10³)	Sonic Mod. psi (×10⁻⁶)	Compr. Str. psi (×10⁻³)	Ult. Str. psi (×10⁻³)
315-21D	2000	1.01	--	--	--	--	--	2.70	7.62
315-22	2000	0.90	1.63	--	--	--	--	--	--
315-24	2000	1.15	1.78	--	--	--	--	--	--
315-25A	2000	0.88	--	--	--	--	--	24.3	4.61
315-25B	2000	0.87	--	--	--	--	--	--	4.78
315-25C	2000	0.88	1.41	.317	--	2.38	1.55	35.5	7.38
315-26B	2000	0.88	--	--	--	--	--	30.5	6.63
315-26C	2000	0.80	1.45	.057	--	--	1.20	25.6	4.24
315-26D	2000	0.83	1.45	.149	--	--	1.36	36.6	--
315-28	2000	0.96	1.46	--	--	--	--	37.3	4.39
315-30	2000	0.91	1.49	--	--	--	--	--	--
315-31	2000	0.85	1.48	--	--	--	--	--	--
315-31B	2000	0.80	1.46	.119	--	0.33	1.44	35.1	5.15
315-31C	2000	0.93	1.48	.237	--	0.47	1.65	--	--
315-31D	2000	0.91	1.46	.229	--	0.42	1.60	36.2	6.6
315-32	2000	0.99	1.43	--	--	--	--	45.0	6.35
315-33	2000	0.78	1.50	.195	--	1.50	1.26	21.0	2.95
315-34C	2000	0.60	1.58	.294	--	0.31	0.87	16.4	2.73
315-34D	2000	0.66	1.57	.137	--	2.01	1.22	--	--
315-35B	2000	0.87	1.89	--	--	--	--	--	--
315-37	2000	0.53	1.61	.262	--	0.31	0.61	14.2	2.51
315-38	2000	0.72	1.51	--	--	--	--	--	--
315-38A	2000	0.72	1.51	.237	--	--	0.93	2.40	2.97
315-39A	2000	0.96	1.64	.188	--	0.47	1.78	35.9	5.59
315-39B	2000	0.96	1.64	.029	--	1.28	1.76	28.5	4.41
315-40	2000	0.87	1.33	--	--	--	--	--	--
315-41	2000	0.68	1.67	.220	--	--	--	15.0	--
315-41A	2000	0.77	1.67	.038	--	1.18	1.35	18.6	2.0
315-41B	2000	0.79	1.67	.157	--	0.98	1.28	16.0	2.02
315-42	2000	0.87	1.83	.249	--	0.35	1.65	--	--
315-43	2000	1.04	1.90	--	--	--	--	50.0	--
315-44	2000	0.76	1.78	.214	--	0.32	1.43	--	--
315-45	2000	0.88	1.66	--	--	--	--	--	--

Sample #	Temp. °C	$\rho_{app.}$ (g/cc)	ρ_{He} (g/cc)	Resistivity Ω-cm (×10)	Hard-ness (DPH)	Int. Frict. (×10³)	Sonic Mod. psi (×10⁻⁶)	Compr. Str. psi (×10⁻³)	Ult. Str. psi ×10⁻³
315-45B	2000	0.76	1.39	.039	--	0.28	5.8	--	--
315-46	2000	1.094	--	--	240	--	--	--	--
315-46	2000	1.094	--	--	105	--	--	--	--
315-46A	2000	0.899	1.55	--	58	--	--	2.5	2.23
317-1	2000	1.21	1.67	--	--	--	--	56.5	7.5
317-2	2000	0.71	1.74	.088	--	--	0.91	23.7	2.97
317-5	2000	0.78	1.42	--	58	--	--	33.1	7.50
317-6	2000	0.78	1.88	--	--	--	--	--	--
317-7	2000	0.79	1.82	--	--	--	--	--	--
317-8	2000	0.90	1.64	--	--	--	1.82	40.5	2.29
317-9	2000	0.93	1.76	--	--	--	--	32.3	5.77
317-10	2000	0.79	1.42	.009	--	0.75	1.45	43.7	6.00
317-12	2000	0.89	1.60	--	--	--	--	--	5.82
317-13	2000	0.88	1.88	--	--	--	--	--	--
317-14	2000	0.87	1.49	--	--	--	--	27.4	4.69
317-15	2000	0.91	1.46	--	--	--	--	33.6	4.09
317-18	2000	0.72	1.50	.088	--	0.39	0.86	5.1	3.30
317-19	2000	1.13	1.68	--	--	--	--	28.2	8.75
317-20	2000	1.05	1.51	--	--	--	--	--	--
317-23	2000	0.83	--	--	--	--	--	7.6	1.90
317-24	2000	0.76	1.57	.187	--	0.76	1.45	49.1	4.37
317-25	2000	0.88	1.69	--	--	--	--	34.1	2.85
317-26	2000	0.78	1.48	.195	14	0.66	1.51	4.7	0.92
317-27	2000	--	--	--	--	--	--	37.3	--
317-28	2000	0.93	1.7	--	--	--	--	--	--
317-29	2000	0.74	1.65	.122	--	--	0.86	16.4	2.48
317-30	2000	0.77	1.68	--	--	--	--	--	--
317-31	2000	0.70	1.45	--	--	--	--	--	--
317-32	2000	0.89	1.72	.224	--	--	1.64	44.2	5.05
317-33	2000	1.02	1.46	--	73	--	--	40.2	5.60
317-34	2000	0.65	1.56	.321	--	--	2.07	24.0	4.61
317-35	2000	0.98	1.40	--	--	--	--	--	--
317-37	2000	0.90	1.34	.225	80	0.31	1.61	40.6	6.90

Sample #	Temp.°C	$\rho_{app.}$ (g/cc)	ρ_{He} (g/cc)	Resistivity Ω-cm(×10)	Hardness (DPH)	Int. Frict.(×10³)	Sonic Mod. psi(×10⁻⁶)	Compr. Str. psi(×10⁻³)	Ult. Str. psi(×10⁻³)
317-38	2000	0.92	1.34	.268	62	1.27	1.01	37.6	4.20
317-39	2000	0.77	1.27	.032	49	0.19	1.20	26.7	3.58
317-40	2000	0.86	1.47	.184	--	--	1.25	22.8	3.44
317-41	2000	0.93	--	--	--	--	--	10.0	2.35
317-41A	2000	0.90	--	--	--	--	--	7.4	1.91
317-41B	2000	1.12	1.48	--	--	--	--	27.0	3.90
317-42	2000	0.87	1.45	.135	53	--	1.54	39.8	5.30
317-43	2000	0.90	1.40	--	--	--	--	15.0	2.47
317-44	2000	0.84	1.51	.007	52	1.68	1.35	27.3	2.13
317-45	2000	0.88	1.40	--	--	--	--	32.3	5.2
317-46	2000	0.81	1.48	.112	71	--	1.27	34.6	4.95
317-47	2000	0.97	1.39	--	49	--	--	27.5	5.62
317-48	2000	1.16	1.46	--	--	--	1.23	--	--
317-49	2000	0.80	1.51	.34	--	1.31	0.89	11.1	3.0
318-1	2000	0.79	1.51	.169	--	--	0.71	--	2.56
318-2	2000	0.95	1.45	--	--	--	--	--	--
318-2C	680	0.89	--	907.0	--	--	0.80	34.5	4.77
318-3	2000	--	1.37	--	--	--	--	--	--
318-6A	2000	1.17	1.45	--	--	--	--	--	--
318-7	2000	0.78	--	--	--	--	0.65	0.82	1.67
318-8	2000	0.96	1.49	.165	60	--	--	18.2	5.62
318-8A	2000	0.97	--	--	--	--	--	32.7	--
318-9	2000	0.96	1.50	--	56	--	--	27.4	5.19
318-10	2000	0.99	1.48	--	--	--	--	--	--
318-11	2000	0.91	1.58	--	51	--	1.48	--	5.09
318-12	2000	0.98	1.50	--	61	--	--	--	--
318-13	2000	1.03	--	--	71	--	--	--	--
318-14	2000	0.77	1.47	.285	31	0.41	0.41	4.74	0.83
318-15	2000	0.95	1.51	--	40	--	--	--	--
318-16	2000	0.94	1.48	.270	47	--	1.43	28.2	4.02
318-17	2000	0.74	1.46	.189	53	0.18	1.18	33.2	4.35
318-18	2000	--	1.48	--	46	--	--	--	--
318-18B	2000	--	--	--	--	--	--	--	5.28

Sample #	Temp.°C	$\rho_{app.}$ (g/cc)	ρ_{He} (g/cc)	Resistivity Ω-cm(×10)	Hard-ness (DPH)	Int. Frict. (×10³)	Sonic Mod. psi×10⁻⁶	Compr. Str. psi ×10⁻³	Ult. Str. psi ×10⁻³
318-19	2000	0.77	1.41	--	--	--	--	--	--
318-20	2000	--	1.50	--	65	--	--	--	--
318-21	2000	--	1.37	--	56	--	--	--	--
318-22	2000	0.83	1.45	.237	44	--	1.29	29.5	4.37
318-22	700	0.78	1.48	--	39	--	--	--	--
318-23	2000	0.91	1.49	--	54	--	--	--	--
318-24	2000	0.97	1.29	--	61	--	1.49	--	4.47
318-24C	2000	0.96	--	--	--	--	--	25.0	--
318-26	2000	0.98	1.59	--	70	--	--	--	--
318-27	2000	0.87	1.38	--	--	--	--	--	--
318-28	2000	0.84	1.45	.177	--	--	1.33	--	0.73
318-29	2000	0.63	1.45	.194	26	--	--	0.23	5.82
318-30	2000	1.08	1.49	--	60	--	1.52	21.9	0.19
318-31	2000	0.55	1.31	.216	21	2.41	0.135	1.6	--
318-32	2000	0.84	1.57	--	53	--	--	19.7	--
318-33	2000	0.80	--	.101	57	0.73	1.37	32.2	4.75
318-34	2000	1.09	1.45	--	--	--	--	28.7	4.85
318-35	2000	0.88	1.43	1.18	--	--	1.48	26.4*	4.57
318-36	2000	1.03	1.41	1.07	67	--	1.35	18.6*	3.34
318-37	2000	0.92	1.48	1.12	--	--	2.17	25.7*	3.90
318-38	2000	--	1.52	--	--	--	--	--	--
318-39	2000	1.24	1.57	.85	--	--	2.99	34.9*	7.95
318-41	2000	1.05	1.44	--	--	--	--	--	--
318-43	2000	1.08	--	--	106	--	--	--	--
318-44	2000	1.09	--	--	103	--	--	--	--
318-45	2000	1.27	--	.39	--	--	3.1	--	--
318-46	2000	1.02	--	.41	56	--	2.34	42.3*	7.35
318-48	2000	1.04	1.43	--	--	--	--	3.5	8.27
318-50	2000	--	--	--	--	--	--	--	5.73
318-51	2000	0.88	1.43	--	--	--	0.83	17.3	1.44

*Head Speed .05 in/min., all others .02 in/min.

Sample #	Temp.°C	$\rho_{app.}$ (g/cc)	ρ_{He} (g/cc)	Resistivity Ω-cm(×10)	Hard-ness (DPH)	Int. Frict.(×10³)	Sonic Mod. psi (×10⁻⁶)	Compr. Str. psi (×10⁻³)	Ult. Str. psi (×10⁻³)
318-52	2000	1.01	1.41	1.30	--	--	1.66	17.7	2.54
318-53	2000	0.87	1.42	--	--	--	--	4.73	1.60
318-56	2000	0.85	1.34	--	--	--	--	--	--
318-58	2000	0.98	--	2.37	--	--	0.10	--	6.02
318-59	2000	1.18	1.38	--	--	--	2.15	31.7	4.20
318-60	2000	0.95	1.71	1.50	54	--	1.78	36.2*	7.63
318-61	2000	1.01	1.75	.403	--	--	1.47	22.6*	3.96
318-62	2000	0.96	1.39	--	69	--	--	41.4	6.98
321-1B	2000	--	--	--	--	--	--	4.36	.87
321-3	2000	0.95	1.57	.340	78	--	--	40.0*	7.18
321-5	2000	0.99	1.52	--	--	--	--	--	--
321-6	2000	1.09	1.60	.31	81	--	2.33	41.7*	8.27
321-7	2000	0.91	1.54	--	--	--	--	--	--
321-8	2000	0.90	1.46	.546	105	--	1.48	38.9*	7.00
321-9	2000	1.17	1.36	--	120	--	--	54.2	9.75
321-10	2000	1.26	1.34	1.00	99	--	2.99	54.9*	10.85
321-11	2000	0.95	1.43	1.14	95	--	1.54	40.5	5.16
321-11C	2000	--	--	--	132	--	--	37.0	6.08
321-12	2000	0.97	1.32	1.21	--	--	1.22	14.9	2.52
321-13	2000	0.95	1.48	1.15	131	--	1.67	36.2	6.04
321-15	2000	0.96	1.56	--	--	--	--	34.5	5.98
321-16A	2000	0.85	1.84	--	--	0.21	1.55	24.3	4.52
321-16B	2000	0.93	1.75	--	--	--	--	--	--
321-17B	2000	0.94	1.41	--	--	0.22	1.81	36.7	5.26
321-18A	2000	0.95	1.67	--	--	--	--	--	--
321-18B	2000	0.64	--	--	--	0.2	--	--	--
321-19A	2000	0.87	1.68	--	115	0.15	1.73	39.6	5.67
321-19B	2000	0.83	1.80	--	87	0.11	1.83	31.5	6.04
321-20A	2000	0.99	1.72	--	--	--	1.49	31.4	5.76
321-20B	2000	0.70	1.50	--	--	--	--	34.8	6.21
321-21A	2000	0.94	1.74	.2	--	--	1.65	45.5	6.35

*Head Speed .05 in/min., all others .02 in/min.

Sample #	Temp. °C	$\rho_{app.}$ (g/cc)	ρ_{He} (g/cc)	Resistiv.ty Ω-cm (×10)	Hard-ness (DPH)	Int. Frict. (×10³)	Sonic Mod. psi (×10⁻⁶)	Compr. Str. psi (×10⁻³)	Ult. Str. psi (×10⁻³)
321-21B	2000	1.00	2.18	.2	--	--	1.93	46.4	6.16
321-22A	2000	0.94	1.79	.28	--	--	1.44	31.9	6.14
321-22B	2000	0.98	--	--	--	--	--	34.8	4.58
321-22C	2000	0.98	--	.17	--	--	1.43	36.1	4.35
321-22D4	2000	0.96	--	.19	--	--	1.42	33.7	5.15
321-23	2000	1.04	1.74	.12	--	--	2.05	58.6	7.28
321-23A	2000	0.96	--	.27	--	--	1.64	40.9	6.36
321-23B	2000	0.97	1.77	.18	--	--	1.69	42.7	5.98
321-24	2000	0.92	--	.19	--	--	1.95	47.8	6.39
321-24A	2000	0.92	--	.14	--	--	1.05	49.1	7.04
321-24B	2000	1.07	2.08	.15	--	--	2.22	45.1	6.76
321-25A	2000	1.05	1.45X*	.13	--	--	0.68	27.9	5.14
321-26	2000	0.50	1.43	--	--	--	--	26.4	0.77
321-26A	2000	0.45	1.54	--	--	--	--	--	--
321-27	2000	0.86	1.52	.11	--	--	0.62	9.7	1.34
321-29	2000	0.96	1.64	.18	--	--	1.59	40.0	5.94
321-31	2300	0.81	1.41	--	--	--	--	--	--
321-31A	2300	0.97	1.40	--	--	--	--	--	--
321-31B	2300	0.91	1.56	--	--	--	--	--	--
321-31C	2300	0.88	1.41	--	--	--	--	--	--
321-31D	2300	--	1.98	--	--	--	--	--	--
321-31F	2300	0.75	--	.23	--	--	0.70	33.3	4.08
321-31G	2300	1.03	1.66	.18	--	--	--	13.6	2.23
321-31I	2300	1.02	1.48	--	--	--	--	22.2	3.53
321-31J	2000	0.99	--	.16	--	--	1.15	22.6	3.99
321-31P	2000	0.93	--	.24	--	--	1.16	25.0	3.60
321-31Q	2000	1.01	1.29	.17	--	--	1.64	40.5	6.23
321-31R	2000	0.93	--	.18	--	--	0.85	12.2	1.85
321-31S	2000	1.01	1.39	.17	--	--	1.53	36.9	5.58
321-32A	2000	0.94	1.36	.18	--	--	0.91	35.5	3.78
321-32B	2000	0.96	1.30	.20	--	--	0.92	36.9	5.76

*Xylene, all others Helium.

Sample #	Temp. °C	$\rho_{app.}$ (g/cc)	ρ_{He} (g/cc)	Resistivity Ω-cm ($\times 10$)	Hardness (DPH)	Int. Frict. ($\times 10^3$)	Sonic Mod. psi $\times 10^{-6}$	Compr. Str. psi ($\times 10^{-3}$)	Ult. Str. psi ($\times 10^{-3}$)
321-32C	2000	0.95	1.25	.21	--	--	0.93	41.4	6.11
321-32D	2000	0.94	--	.25	--	--	1.49	--	--
321-32D₁	2000	0.94	--	.29	--	--	0.2	--	--
321-32E	2000	0.98	1.33	.24	--	--	1.56	41.9	5.89
321-32F	2000	0.96	--	--	--	--	0.91	33.3	4.28
321-32G	2000	0.99	--	.22	--	--	1.56	31.8	4.53
321-33A	2000	0.97	1.41	.16	--	--	--	39.8	5.96
321-33B	2000	0.89	1.30	.33	--	--	--	53.6	6.69
321-34	2300	0.95	1.6	--	--	--	--	--	--
321-34A	2300	0.92	1.59	.27	--	--	1.49	31.3	7.55
321-34B	2300	0.96	--	.18	--	--	2.94	33.3	2.92
321-34D	2300	0.99	--	--	--	--	1.46	--	--
321-34E₁	2300	0.97	1.21	.38	--	--	0.92	40.9	5.43
321-36A	2300	1.11	1.80	--	--	--	--	--	2.46
321-36B	2300	1.07	1.66	.29	--	--	1.15	50.4	7.23
321-36C	2300	1.11	1.43	--	--	--	--	--	--
321-37	2300	1.07	1.44	--	--	--	--	--	--
321-37B	2300	0.66	1.50	.24	--	--	0.42	5.53	1.09
321-37D₁	2300	--	--	--	--	--	--	2.51	0.45
321-37E	2300	0.78	1.56X	.44	--	--	0.94	1.39	0.36
321-37F	2300	0.68	--	--	--	--	0.08	1.05	0.22
321-37Q	2300	0.74	--	.31	--	--	0.2	1.67	0.40
321-39	2300	0.85	1.60	.23	--	--	0.72	6.80	1.31
321-40	2300	0.60	1.42	.30	--	--	--	--	--
321-41B	2300	0.77	1.51	--	--	--	--	--	--
321-42A	2000	0.77	1.44X	.29	--	--	0.35	2.05	0.57
321-42B	2000	0.65	1.48	.28	--	--	0.20	1.14	0.42
321-43A	2200	0.76	1.55	.36	--	--	0.60	1.31	0.37
321-43B	2200	0.64	1.44	.46	--	--	0.10	0.73	0.22
321-44A	2200	0.96	1.81	--	--	--	--	--	--
321-44B	2200	0.98	1.56	--	--	--	--	--	--
321-45A	2200	1.17	1.78	--	--	--	--	--	--
321-45B	2200	1.04	1.84	--	--	--	--	--	--

Sample #	Temp.°C	$\rho_{app.}$ (g/cc)	ρ_{He} (g/cc)	Resistivity Ω-cm($\times$10)	Hardness (DPH)	Int. Frict. ($\times 10^3$)	Sonic Mod. psi ($\times 10^{-6}$)	Compr. Str. psi ($\times 10^{-3}$)	Ult. Str. psi ($\times 10^{-3}$)
321-46A	2200	0.83	1.40	--	--	--	--	--	--
321-46B	2200	0.82	1.43	.26	--	--	--	--	--
321-46C	2200	0.87	1.60	--	--	--	0.16	2.04	0.49
321-47A	1600	1.13	2.07	--	--	--	--	--	--
321-47B	1600	1.18	1.67	--	--	--	--	--	--
321-47C	1600	0.91	1.84	--	--	--	--	--	--
321-48A	1600	0.79	1.40	--	--	--	--	--	--
321-48B	1600	0.83	1.43	.24	--	--	--	--	--
321-48C	2000	0.78	1.58	--	--	--	0.34	2.65	0.60
321-49A	1600	0.91	1.51	--	--	--	--	--	--
321-49B	1600	0.80	1.44	--	--	--	--	--	--
321-49C	1600	0.91	1.51	--	--	--	--	--	--
321-50	1600	1.00	1.69	--	--	--	--	--	--
321-50B	1600	1.02	1.43	.15	--	--	1.5	28.2	4.52
321-50C	1600	1.03	1.45	--	--	--	--	--	--
321-51	2350	0.99	1.50	--	--	--	0.73	9.1	1.36
321-51A	2350	1.01	1.53	.21	--	--	--	--	--
321-52	2000	--	1.3	--	--	--	--	--	--
321-53	2000	1.12	2.07	--	--	--	--	--	--
322-1A	1600	0.77	1.59X	.24	--	--	--	--	--
322-1B	1600	0.77	1.98	.39	--	--	--	4.00	0.78
322-2A	1600	0.87	2.02	--	--	--	--	--	--
322-3A	1600	0.78	1.59X	.18	--	--	0.73	--	--
322-3B	1600	0.78	2.0	--	--	--	--	--	--
322-5	2000	0.86	1.55	--	--	--	--	--	--
322-6	2000	0.86	1.41	--	--	--	--	--	--
322-10C	2100	0.84	1.8	--	--	--	--	--	--
322-11A	1670	0.78	1.49X	--	--	--	0.25	--	--
322-11B	1670	0.78	1.9	.26	--	--	0.24	--	--
322-12A	1600	0.71	1.43X	.28	--	--	0.24	--	--
322-12B	1600	0.79	1.50X	.23	--	--	0.35	--	--
322-13A	1670	0.79	1.45X	.17	--	--	0.59	--	--
322-14A	1670	0.76	1.74	--	--	--	--	--	--

Sample #	Temp.°C	$\rho_{app.}$ (g/cc)	ρ_{He} (g/cc)	Resistivity Ω-cm(×10)	Hardness (DPH)	Int. Frict. (×10³)	Sonic Mod. psi (×10⁻⁶)	Compr. Str. psi (×10⁻³)	Ult. Str. psi (×10⁻³)
322-15B	1670	0.86	1.48X	.19	--	--	0.57	--	--
322-16A	1670	0.81	1.89	--	--	--	--	--	--
322-16B	1670	0.84	1.81X	.22	--	--	0.35	--	--
322-17B	1670	0.76	1.71X	.37	--	--	0.2	--	--
322-18A	1670	1.01	--	.09	--	--	2.17	--	--
322-19A	1670	0.85	1.9	--	--	--	--	--	--
322-19B	1670	0.89	--	.28	--	--	0.33	--	--
322-20	1400	0.89	--	.17	--	--	0.77	--	--
322-21	1400	0.81	--	.22	--	--	0.53	--	--
322-22A	1400	0.88	1.49X	--	--	--	--	4.1	1.19
322-22B	1400	0.89	--	--	--	--	--	5.2	1.19
322-23A	1400	0.84	--	--	--	--	--	--	--
322-23B	1300	0.83	2.03X	--	--	--	--	--	4.07
322-24A	1300	0.87	1.74X	--	--	--	--	--	1.28
322-24B	1400	0.82	1.59X	--	--	--	--	--	1.28
322-25A	1410	0.88	--	.11	--	--	1.56	--	--
322-25A	1670	0.88	--	.13	--	--	1.48	--	--
322-26	1400	1.00	--	.11	--	--	2.04	--	--
322-27A	1400	0.86	1.42X	.08	--	--	1.58	--	3.16
322-28A	1400	0.93	1.44X	.10	--	--	--	18.4	--
322-29A	1400	0.69	1.46X	.19	--	--	0.68	--	--
322-30	1410	0.92	1.64	.18	--	--	0.79	--	--
322-31B	1410	0.75	1.58X	.34	--	--	0.24	--	--
322-32	1350	0.79	1.60X	.24	--	--	0.36	5.8	0.79
322-33	1350	0.79	1.78X	.22	--	--	0.60	--	--
322-34	1350	0.88	1.34X	.13	--	--	1.07	--	--
322-35	1350	0.86	1.43X	.22	--	--	0.68	11.8	1.33
322-36	1543	0.93	1.45X	.10	--	--	1.29	23.0	3.74
322-37	1543	0.82	1.46X	.20	--	--	0.47	--	--
322-38	1543	0.72	--	.17	--	--	0.93	--	--
322-39	1440	0.84	--	.18	--	--	0.72	--	--
322-40	1440	0.87	1.86X	.11	--	--	1.14	--	--
322-41	1440	0.79	1.59X	.17	--	--	0.84	--	--

Sample #	Temp.°C	$\rho_{app.}$ (g/cc)	ρ_{He} (g/cc)	Resistivity Ω-cm(×10)	Hardness (DPH)	Int. Frict. (×10³)	Sonic Mod. psi (×10⁻⁶)	Compr. Str. psi (×10⁻³)	Ult. Str. psi (×10⁻³)
322-42A$_3$	1440	0.78	--	.14	--	--	0.88	--	--
322-42A$_4$	1440	0.73	--	.23	--	--	0.68	--	--
322-42B$_1$	1440	0.73	--	.20	--	--	0.69	--	--
322-42B$_2$	1440	0.78	--	.18	--	--	0.87	--	--
322-42B$_3$	1440	0.80	--	.27	--	--	0.89	19.4	3.11
322-42B$_4$	1440	0.73	--	.17	--	--	0.70	--	--
322-42B$_5$	1440	0.74	--	.19	--	--	0.76	--	--
322-42B$_6$	1440	0.83	--	.19	--	--	0.97	--	--
322-45	1440	0.91	1.72X	.20	--	--	0.68	--	--
322-48	1605	0.73	--	.29	--	--	0.43	--	--
322-49A	1605	0.79	1.51x	.15	--	--	0.79	--	--
322-50	1600	0.79	--	.15	--	--	0.56	--	--
322-51	1460	0.78	1.56	--	--	--	--	--	--
322-56	1500	1.00	1.48	--	--	--	--	--	--
322-56A	1500	0.96	1.33	--	--	--	--	--	--
322-57	1500	1.06	1.63	--	--	--	--	--	--
322-57A	1500	1.03	1.85	--	--	--	--	--	--
322-61	1500	0.79	1.50	--	--	--	0.4	--	--
322-62	1500	1.01	1.62	--	--	--	1.21	--	--
322-63	1500	1.03	1.56	--	--	--	1.69	--	--
322-63A	1500	1.12	1.49	--	--	--	2.47	--	--
322-64	1370	1.00	1.60	--	--	--	1.92	--	--
322-64A	1370	1.10	1.55	--	--	--	1.92	--	--
322-64B	1370	0.97	1.61	--	--	--	1.89	--	--
322-65	1370	1.28	1.45	--	--	--	--	--	--
322-66	1370	1.09	1.37	--	--	--	--	--	--
322-67	1350	0.85	1.64	--	--	--	1.32	--	--
322-67A	1370	0.84	1.65	--	--	--	--	--	--
322-67B	1370	0.86	1.84	--	--	--	1.33	--	--
322-68	1370	0.78	1.52	--	--	--	0.53	--	--
322-68A	1370	0.79	1.25	--	--	--	--	--	--
322-68B	1370	0.77	1.48	--	--	--	--	--	--
322-69	1370	0.76	1.50	--	--	--	0.42	--	--

Sample #	Temp.°C	$\rho_{app.}$ (g/cc)	ρ_{He} (g/cc)	Resistivity Ω-cm(×10)	Hard-ness (DPH)	Int. Frict. (×10³)	Sonic Mod. psi (×10⁻⁶)	Compr. str. psi (×10⁻³)	Ult. str. psi (×10⁻³)
322-69A	1370	0.76	1.56	--	--	--	0.42	--	--
322-70	1370	0.69	1.56	--	--	--	0.38	--	--
323-1	1370	1.01	1.47	--	--	--	--	--	--
323-2	1370	0.81	1.51	--	--	--	1.15	--	--
323-2A	1370	0.73	1.50	--	--	--	1.30	--	--
323-3	1370	0.98	1.36	--	--	--	--	--	--
323-3A	1370	1.13	1.61	--	--	--	2.48	--	--
323-4	1370	0.78	1.49	--	--	--	0.55	--	--
323-4A	1370	0.76	1.49	--	--	--	0.55	--	--
323-8A	1000	0.95	1.52	--	--	--	--	--	--

TABLE 9

Physical Properties Correlated with Density

Sample #	$E_s/\rho_{app.}$ in ($\times 10^{-6}$)	$\sigma_{cs}/\rho_{app.}$ in ($\times 10^{-3}$)	$\sigma_{UTS}/\rho_{app.}$ in ($\times 10^{-3}$)	$E_s\left(\frac{\rho_{He}}{\rho_{app.}}\right)$ psi ($\times 10^{-6}$)	$\sigma_{cs}\left(\frac{\rho_{He}}{\rho_{app.}}\right)$ psi ($\times 10^{-3}$)	$\sigma_{UTS}\left(\frac{\rho_{He}}{\rho_{app.}}\right)$ psi ($\times 10^{-3}$)	$\rho\left(\frac{\rho_a}{\rho_{He}}\right)$ Ω-cm ($\times 10$)
310-35	--	252.4	49.2	--	--	--	--
311-34	--	333.3	325.9	--	--	--	--
311-35	19.2	37.2	66.9	--	--	--	--
312-13	--	1298.0	125.9	--	--	--	--
312-14	--	1000.0	--	--	--	--	--
312-16	--	624.0	102.1	--	51.8	4.67	--
312-27	--	--	188.0	--	28.5	--	--
312-29	--	1030.6	--	--	--	--	--
312-32	--	901.2	158.3	--	56.4	8.38	--
312-34	--	824.2	33.5	--	47.7	1.09	--
312-49	--	--	150.5	--	40.9	7.04	--
315-2	50.3	58.5	14.3	2.76	3.2	0.78	.016
315-14	--	1235.5	136.0	--	--	--	--
315-17	--	1030.0	88.3	--	71.2	1.04	--
315-20A	48.8	--	--	2.82	--	--	--
315-20B	49.3	--	--	2.85	--	--	.013
315-20C	48.1	--	--	2.76	--	--	.009
315-21B	--	--	191.0	--	--	--	--
315-21C	45.8	1428.6	217.6	2.51	--	11.9	.009
315-21D	--	743.0	209.5	--	78.2	--	--
315-25A	--	767.0	145.5	--	--	--	.009
315-25B	--	--	152.6	--	--	--	--
315-25C	48.8	1120.5	232.9	2.41	56.9	11.8	.020
315-26B	--	962.8	209.3	--	--	--	--
315-26C	41.7	888.9	147.2	2.18	46.4	7.7	.003
315-26D	46.2	1224.9	--	2.34	63.9	--	.009
315-28	--	1079.3	127.0	--	56.7	6.68	--
315-31B	50.0	1213.8	178.8	2.63	63.4	9.4	.007
315-31C	49.3	--	--	2.63	--	--	.015
315-31D	48.8	1105.0	201.5	2.56	58.1	10.6	.014
315-32	--	1262.6	178.2	--	65.0	9.2	--

Sample #	$E_s/\rho_{app.}$ in($\times 10^{-6}$)	$\sigma_{cs}/\rho_{app.}$ in($\times 10^{-3}$)	$\sigma_{UTS}/\rho_{app.}$ in($\times 10^{-3}$)	$E_s\left(\dfrac{\rho_{He}}{\rho_{app.}}\right)$ psi($\times 10^{-6}$)	$\sigma_{cs}\left(\dfrac{\rho_{He}}{\rho_{app.}}\right)$ psi($\times 10^{-3}$)	$\sigma_{UTS}\left(\dfrac{\rho_{He}}{\rho_{app.}}\right)$ psi($\times 10^{-3}$)	$\rho\left(\dfrac{\rho_a}{\rho_{He}}\right)$ Ω-cm($\times 10$)
315-33	44.9	--	--	2.42	--	--	.010
315-34C	40.3	972.2	136.6	2.29	55.3	7.7	.011
315-34D	51.5	690.2	114.9	2.91	39.0	6.5	.006
315-37	31.9	744.2	131.6	1.85	43.1	7.6	.009
315-38A	35.9	925.9	114.6	1.95	50.3	6.2	.011
315-39A	51.5	1038.8	161.7	3.03	61.3	9.5	.011
315-39B	51.0	824.7	127.6	3.01	48.7	7.5	.002
315-41	--	--	--	--	--	--	.009
315-41A	48.7	612.8	72.2	2.93	36.8	4.3	.002
315-41B	45.9	671.0	69.9	2.69	40.3	4.3	.007
315-42	52.7	563.0	--	3.47	33.8	--	.012
315-43	--	--	--	--	--	--	--
315-44	52.1	1335.5	--	3.34	91.3	--	.009
315-45B	211.9	--	--	10.6	--	--	.002
315-46A	--	2.78	2.48	--	4.4	3.9	--
317-1	--	1297.1	172.2	--	77.9	10.4	--
317-2	35.6	922.0	116.2	2.23	55.1	7.3	.004
317-5	--	1175.0	266.0	--	56.1	13.7	--
317-8	56.2	1247.0	70.5	3.32	73.8	4.17	--
317-9	--	964.8	172.3	--	61.1	10.9	.001
317-10	50.9	1536.6	210.9	2.61	78.5	10.8	--
317-12	--	--	181.6	--	--	10.5	--
317-14	--	874.8	149.7	--	46.9	8.03	--
317-15	--	1025.6	124.8	--	53.9	6.6	.004
317-18	33.0	126.0	104.0	1.79	10.6	6.9	--
317-19	--	693.2	215.1	--	41.9	13.0	.009
317-23	--	254.0	63.4	--	--	--	--
317-24	52.9	1794.6	159.7	2.99	101.4	9.0	.010
317-25	--	1076.4	89.9	--	65.5	5.5	.009
317-26	53.7	167.4	32.8	2.86	8.9	1.7	.012
317-29	32.3	615.0	92.8	1.92	36.6	5.53	--
317-32	51.3	1380.0	113.0	3.17	85.4	7.0	--
317-33	--	1092.0	152.0	--	57.5	8.0	--

Sample #	$E_s/\rho_{app.}$ in($\times 10^{-6}$)	$\sigma_{cs}/\rho_{app.}$ in($\times 10^{-3}$)	$\sigma_{UTS}/\rho_{app.}$ in($\times 10^{-3}$)	$E_s\left(\frac{\rho_{He}}{\rho_{app.}}\right)$ psi($\times 10^{-6}$)	$\sigma_{cs}\left(\frac{\rho_{He}}{\rho_{app.}}\right)$ psi($\times 10^{-3}$)	$\sigma_{UTS}\left(\frac{\rho_{He}}{\rho_{app.}}\right)$ psi($\times 10^{-3}$)	$\rho\left(\frac{\rho_a}{\rho_{He}}\right)$ Ω-cm($\times 10$)
317-34	88.4	1025.6	197.0	4.97	57.6	11.1	.013
317-37	49.8	1049.0	212.0	2.40	60.4	10.3	.015
317-38	31.3	1158.0	126.0	1.47	54.76	6.11	.018
317-39	43.3	963.0	129.0	1.98	44.0	5.9	.002
317-40	40.7	736.0	111.0	2.15	38.9	5.9	.011
317-41	--	298.0	70.0	--	--	--	--
317-41A	--	228.0	58.8	--	--	--	--
317-41B	--	668.0	96.5	--	35.7	5.15	--
317-42	49.1	1266.0	169.0	2.63	66.3	8.8	.008
317-43	--	462.0	76.0	--	23.4	3.84	--
317-44	44.6	903.0	70.4	2.43	4.91	3.83	.0004
317-45	--	1017.0	164.0	--	51.4	8.3	--
317-46	43.5	1183.0	215.0	2.32	63.2	9.7	.006
317-47	--	785.0	160.0	--	39.3	8.05	--
317-48	29.9	--	--	1.57	--	--	--
317-49	30.8	385.4	104.2	1.67	20.9	5.7	.018
318-1	24.8	--	89.8	1.35	--	4.9	.009
318-2C	25.0	1076.8	148.9	--	--	--	--
318-7	23.2	29.2	28.0	--	--	--	--
318-8	--	526.6	162.6	--	28.2	8.7	--
318-8A	--	936.4	--	--	--	--	--
318-9	--	792.8	150.2	--	42.8	8.1	--
318-11	45.3	--	155.0	2.58	9.0	8.8	--
318-14	14.6	170.9	29.9	.76	44.4	1.6	.015
318-16	42.3	831.0	118.0	2.26	65.5	2.3	.017
318-17	44.2	1246.2	163.0	2.66	51.5	8.51	.019
318-22	43.2	987.0	146.0	2.25	--	7.63	.014
318-24	42.5	--	--	1.97	--	--	--
318-24C	--	715.0	129.0	--	--	--	--
318-28	43.9	--	--	2.30	--	--	.010
318-29	--	10.1	32.2	--	.5	1.7	.008
318-30	39.2	563.3	149.62	2.10	30.2	8.03	--
318-31	6.8	80.3	9.6	.32	3.8	.5	.009

Sample #	$E_s/\rho_{app.}$ in($\times10^{-6}$)	$\sigma_{cs}/\rho_{app.}$ in($\times10^{-3}$)	$\sigma_{UTS}/\rho_{app.}$ in($\times10^{-3}$)	$E_s\left(\dfrac{\rho_{He}}{\rho_{app.}}\right)$ psi($\times10^{-6}$)	$\sigma_{cs}\left(\dfrac{\rho_{He}}{\rho_{app.}}\right)$ psi($\times10^{-3}$)	$\sigma_{UTS}\left(\dfrac{\rho_{He}}{\rho_{app.}}\right)$ psi($\times10^{-3}$)	$\rho\left(\dfrac{\rho_a}{\rho_{He}}\right)$ Ω-cm($\times10$)
318-32	--	650.0	--	--	36.5	--	--
318-33	46.9	1118.1	164.9	--	--	--	--
318-34	--	729.0	123.0	--	38.2	1.13	--
318-35	46.9	831.0	144.0	2.41	42.9	7.4	.070
318-36	42.6	573.0	103.0	2.12	29.13	5.2	.078
318-37	65.7	773.0	117.0	3.50	41.3	6.3	.070
318-39	64.9	778.0	178.0	3.7	44.2	10.1	.007
318-45	67.6	--	--	--	--	--	--
318-46	62.7	1149.0	200.0	--	--	--	--
318-48	--	93.2	220.0	--	4.9	--	--
318-51	26.0	546.0	45.3	4.23	28.2	2.3	.009
318-52	46.2	486.8	69.9	2.35	24.7	3.55	--
318-53	--	151.0	51.1	--	7.9	2.7	--
318-58	2.8	--	165.0	--	--	--	--
318-59	50.6	744.0	98.6	2.51	39.8	--	--
318-60	52.0	1055.0	222.0	2.2	65.2	13.7	.079
318-61	40.4	620.0	109.0	2.55	39.2	6.9	.023
318-62	--	1195.0	201.0	--	60.2	10.1	--
321-3	--	1166.0	209.0	--	66.1	11.9	--
312-6	59.5	1061.0	210.0	3.43	61.3	12.1	.021
321-8	45.6	1197.0	215.0	2.39	63.1	11.4	.021
321-9	--	1283.0	231.0	--	63.0	11.3	.034
321-10	66.0	1207.0	238.0	3.18	58.4	11.5	--
321-11	44.9	1184.0	151.0	2.36	60.9	7.77	.009
321-12	35.0	427.0	72.0	1.67	20.3	3.4	.076
321-13	48.7	1032.0	176.0	2.59	56.4	9.4	.089
321-15	--	994.00	173.0	--	56.1	9.7	.074
321-16A	50.7	792.0	148.0	3.36	52.6	9.8	--
221-17B	53.5	1089.0	155.0	2.71	55.1	7.9	--
321-18B	80.1	1726.0	246.0	--	--	--	--
321-19A	58.4	1006.0	193.0	3.53	60.8	11.7	--
321-19B	49.9	1055.0	192.0	3.23	68.1	12.5	--
321-20B	--	1381.0	246.4	--	74.6	13.3	--

Sample #	$E_s/\rho_{app.}$ in($\times 10^{-6}$)	$\sigma_{cs}/\rho_{app.}$ in($\times 10^{-3}$)	$\sigma_{UTS}/\rho_{app.}$ in($\times 10^{-3}$)	$E_s\left(\dfrac{\rho_{He}}{\rho_{app.}}\right)$ psi($\times 10^{-6}$)	$\sigma_{cs}\left(\dfrac{\rho_{He}}{\rho_{app.}}\right)$ psi($\times 10^{-3}$)	$\sigma_{UTS}\left(\dfrac{\rho_{He}}{\rho_{app.}}\right)$ psi($\times 10^{-3}$)	$\rho\left(\dfrac{\rho_a}{\rho_{He}}\right)$ Ω-cm($\times 10$)
321-21A	48.8	1344.6	187.6	6.03	86.6	12.1	.011
321-21B	53.6	1288.9	171.1	4.21	101.2	13.4	.009
321-22A	42.6	943.0	181.0	2.74	60.7	11.7	.014
321-22B	--	986.4	129.8	--	54.7	7.2	--
321-22C	40.5	1023.2	123.3	2.2	55.3	6.7	.007
321-22D₄	41.1	975.1	149.0	2.2	51.6	7.9	.010
321-23	54.8	1565.0	194.0	3.4	98.0	12.2	.008
321-23A	47.5	1183.4	184.0	2.6	65.2	10.1	.017
321-23B	48.4	1222.8	171.0	3.1	77.9	10.9	.010
321-24	58.9	1443.0	193.0	3.4	83.1	11.1	.011
321-24A	31.7	1482.5	212.6	--	--	--	--
321-24B	57.6	1170.8	175.5	4.3	87.7	13.1	--
321-25A	18.0	738.0	136.0	.94	38.5	7.10	.009
321-26	--	1466.7	42.8	--	75.5	2.2	.006
321-27	20.0	313.3	43.3	1.2	17.1	2.4	.011
321-29	46.0	1157.0	172.0	2.7	68.3	10.1	.010
321-31F	26.0	503.8	82.6	1.6	30.5	5.0	.011
321-31G	--	599.0	95.2	--	36.0	5.7	.011
321-31J	32.3	634.0	112.0	1.72	33.8	5.96	.018
321-31P	34.6	747.0	108.0	1.56	33.6	4.8	.013
321-31Q	45.1	1114.0	171.0	2.09	51.7	7.96	--
321-31R	25.4	364.4	55.3	--	--	--	.012
321-31S	42.1	1104.9	153.5	2.11	50.8	7.68	.012
321-32A	26.9	1049.0	111.7	1.36	51.4	5.47	.015
321-32B	26.6	1067.7	166.7	1.25	50.0	7.80	.016
321-32C	27.2	1210.5	178.7	1.22	54.5	8.04	--
321-32D	44.0	--	--	--	--	--	--
321-32D₁	5.9	--	--	--	--	--	.018
321-32E	44.2	1187.6	166.1	2.12	56.9	7.99	--
321-32F	26.3	963.5	123.8	1.46	53.4	6.9	--
321-32G	43.8	892.3	127.1	--	--	--	.011
321-33A	--	1139.7	170.7	--	57.9	8.66	--
321-33B	46.5	1673.0	208.8	2.18	78.3	9.77	.023

Sample #	$E_s/\rho_{app.}$ in$(\times 10^{-6})$	$\sigma_{cs}/\rho_{app.}$ in$(\times 10^{-3})$	$\sigma_{UTS}/\rho_{app.}$ in$(\times 10^{-3})$	$E_s\left(\dfrac{\rho_{He}}{\rho_{app.}}\right)$ psi$(\times 10^{-6})$	$\sigma_{cs}\left(\dfrac{\rho_{He}}{\rho_{app.}}\right)$ psi$(\times 10^{-3})$	$\sigma_{UTS}\left(\dfrac{\rho_{He}}{\rho_{app.}}\right)$ psi$(\times 10^{-3})$	$\rho\left(\dfrac{\rho_a}{\rho_{He}}\times 10\right)$ Ω-cm$(\times 10)$
321-34A	45.0	945.0	228.0	2.6	54.1	13.0	.016
321-34B	85.1	963.5	84.5	--	--	--	--
321-34D	41.0	--	--	--	--	--	--
321-34E₁	26.0	1171.2	155.5	1.15	51.0	6.77	.030
321-36A	--	--	61.6	--	--	3.99	--
321-36B	29.9	1308.0	187.7	1.78	78.2	11.2	.019
321-37B	17.7	232.7	45.9	.95	12.6	2.5	.011
321-37E	33.5	49.5	12.8	2.12	3.1	.81	.020
321-37F	3.3	42.9	8.9	.18	2.41	.50	--
321-37Q	7.5	62.7	15.0	.44	3.6	.9	.012
321-39	23.5	222.2	42.8	1.4	12.8	2.5	.013
321-40	--	--	--	--	--	--	.013
321-42A	12.6	73.9	20.6	.65	3.83	1.07	.012
321-42B	8.5	48.7	17.9	4.6	2.6	.96	.012
321-43A	21.9	47.9	13.5	1.2	2.7	.75	.018
321-43B	4.3	31.7	9.5	.23	1.6	.5	.020
321-46B	5.4	69.1	16.6	.28	3.6	.85	.015
321-48B	11.4	88.7	20.0	.6	4.6	1.0	.014
321-50B	40.8	769.9	123.0	2.1	39.5	6.3	.011
321-51	20.5	255.0	38.2	1.1	13.8	2.1	--
321-51A	--	--	--	--	--	--	--
322-1A	9.74	144.3	2.81	.56	8.3	1.6	.014
322-1B	9.38	--	--	.67	--	--	.012
322-3A	26.0	--	--	1.49	--	--	.015
322-11A	8.9	--	--	.48	--	--	.009
322-11B	8.5	--	--	.58	--	--	--
322-12A	9.4	--	--	.48	--	--	.011
322-12B	12.3	--	--	.66	--	--	.014
322-13A	20.7	--	--	1.1	--	--	.012
322-15B	18.4	--	--	.98	--	--	.009
322-16B	11.6	--	--	.75	--	--	.011
322-17B	7.3	--	--	.45	--	--	.010
322-18A	59.7	--	--	--	--	--	.016

Sample #	$E_s/\rho_{app.}$ in($\times10^{-6}$)	$\sigma_{cs}/\rho_{app.}$ in($\times10^{-3}$)	$\sigma_{UTS}/\rho_{app.}$ in($\times10^{-3}$)	$E_s\left(\dfrac{\rho_{He}}{\rho_{app.}}\right)$ psi($\times10^{-6}$)	$\sigma_{cs}\left(\dfrac{\rho_{He}}{\rho_{app.}}\right)$ psi($\times10^{-3}$)	$\sigma_{UTS}\left(\dfrac{\rho_{He}}{\rho_{app.}}\right)$ psi($\times10^{-3}$)	$\rho\left(\dfrac{\rho_a}{\rho_{He}}\right)$ Ω-cm($\times10$)
322-19B	10.3	--	--	--	--	--	--
322-20	24.0	--	--	--	--	--	--
322-21	18.2	--	--	--	--	--	--
322-22A	--	129.4	37.6	--	--	--	--
322-22B	--	162.3	37.1	--	8.71	1.99	--
322-23B	--	--	136.2	--	--	10.20	--
322-24A	--	--	40.9	--	--	2.56	--
322-24B	--	--	60.3	--	--	2.48	--
322-25A	49.2	--	--	--	--	--	--
322-25A	46.7	--	--	--	--	--	--
322-26	56.7	--	--	--	--	--	--
322-27A	51.0	--	--	2.61	--	--	--
322-28A	--	549.6	94.4	--	28.5	4.89	.005
322-29A	27.4	--	--	1.44	--	--	.006
322-30	23.9	--	--	1.41	--	--	.009
322-31B	8.9	--	--	.51	--	--	.010
322-32	12.7	203.9	27.8	.73	11.75	1.6	.016
322-33	21.1	--	--	1.35	--	--	.012
322-34	33.8	--	--	1.63	--	--	.010
322-35	21.9	381.0	43.0	1.13	19.6	2.2	.009
322-36	38.5	686.9	111.7	2.01	35.9	5.83	.013
322-37	15.9	--	--	.84	--	--	.006
322-38	35.9	--	--	--	--	--	.011
322-39	23.8	--	--	--	--	--	--
322-40	36.4	--	--	--	--	--	--
322-41	29.5	--	--	2.44	--	--	.005
322-42A₃	31.3	--	--	1.69	--	--	.008
322-42A₄	25.9	--	--	--	--	--	--
322-42B₁	26.3	--	--	--	--	--	--
322-42B₂	31.0	--	--	--	--	--	--
322-42B₃	31.0	673.6	108.0	--	--	--	--
322-42B₄	26.6	--	--	--	--	--	--
322-42B₅	28.5	--	--	--	--	--	--

Sample #	$E_s/\rho_{app.}$ in($\times 10^{-6}$)	$\sigma_{cs}/\rho_{app.}$ in($\times 10^{-3}$)	$\sigma_{UTS}/\rho_{app.}$ in($\times 10^{-3}$)	$E_s\left(\dfrac{\rho_{He}}{\rho_{app.}}\right)$ psi($\times 10^{-6}$)	$\sigma_{cs}\left(\dfrac{\rho_{He}}{\rho_{app.}}\right)$ psi($\times 10^{-3}$)	$\sigma_{UTS}\left(\dfrac{\rho_{He}}{\rho_{app.}}\right)$ psi($\times 10^{-3}$)	$\rho\left(\dfrac{\rho_a}{\rho_{He}}\right)$ Ω-cm($\times 10$)
322-42B₆	32.5	--	--	--	--	--	--
322-45	20.8	--	--	1.28	--	--	--
322-48	16.4	--	--	--	--	--	.011
322-49A	27.8	--	--	1.51	--	--	--
322-50	19.7	--	--	--	--	--	.008
322-61	14.1	--	--	.8	--	--	--
322-62	33.3	--	--	1.9	--	--	--
322-63	45.6	--	--	2.6	--	--	--
322-63A	61.3	--	--	3.29	--	--	--
322-64	53.3	--	--	3.65	--	--	--
322-64A	48.5	--	--	2.7	--	--	--
322-64B	54.1	--	--	3.14	--	--	--
322-67	43.1	--	--	2.5	--	--	--
322-67B	42.9	--	--	2.8	--	--	--
322-68	18.9	--	--	1.0	--	--	--
322-69	15.4	--	--	.8	--	--	--
322-69A	15.4	--	--	.8	--	--	--
322-70	15.3	--	--	.9	--	--	--
323-2	39.4	--	--	2.1	--	--	--
323-2A	49.5	--	--	2.7	--	--	--
323-3A	61.0	--	--	3.5	--	--	--
323-4	19.6	--	--	1.1	--	--	--
323-4A	20.1	--	--	1.1	--	--	--

TABLE 10   Comparison of Ultimate Strength
Determined by Direct Tension
vs. Disc Rupture

Sample #	Direct Tension	Disc Rupture
317-38	3780 psi	5100 psi
318-59	4600 psi	4153 psi
321-16B	5306 psi	4705 psi
321-36A	4081 psi*	2462 psi
321-50B	3780 psi	5228 psi
322-23B	3163 psi	4050 psi
322-24A	1367 psi	1279 psi
322-24B	1122 psi	1279 psi

*Broke in Grip

TABLE 11   Comparison of Sonic Modulus
and Mechanical Modulus

Sample #	HTT Temp.°C	Mechanical Modulus	Sonic Modulus
317-8	2000	1.27×10^6	1.82×10^6
317-26	2000	0.38×10^6	0.31×10^6
317-42	2000	1.4×10^6	1.5×10^6
317-46	2000	1.59×10^6	1.27×10^6
318-17	2000	1.16×10^6	1.18×10^6
318-52	2000	2.0×10^6	1.69×10^6
321-12	2000	1.01×10^6	1.22×10^6

TABLE 12   Sonic Modulus vs. Pyrolysis
Temperature

psi $(\times 10^{-6})$

Sample #	700°C	800°C	900°C	1000°C	1577°C	1800°C	2000°C
318-59 #1L	1.02	--	--	2.16	1.95	1.77	1.46
318-59 #2L	1.06	--	--	2.07	2.10	1.82	1.76
318-60L	.93	--	--	--	1.82	1.77	1.70
321-11L	.75	--	--	2.37	1.68	1.72	1.58
321-11CL	.73	--	--	1.75	1.75	1.72	1.66
321-12L	.66	--	--	1.49	2.03	1.23	1.18
321-13 #1L	.80	--	--	1.84	1.77	1.73	1.75
321-13 #2L	.82	--	--	1.84	--	1.79	1.72
321-13 #3L	.88	--	--	1.91	--	1.75	1.72
321-15 #1	.81	--	1.69	1.92	1.91	1.84	1.69
321-15 #2	--	1.53	--	1.96	2.01	1.86	1.71
321-15L	--	1.69	--	2.06	1.875	1.86	1.79
321-16A	--	1.60	--	1.88	1.87	1.70	1.55
321-16AL	--	1.57	--	1.97	1.87	1.67	1.58
321-16B	--	1.68	--	1.87	1.68	1.55	1.48
321-17B	.80	--	1.80	2.12	1.96	1.91	1.81
321-18A	--	1.63	--	2.2	2.14	2.09	1.98
321-18B #1	--	1.73	--	1.48	1.86	1.81	1.73
321-18B #2	--	1.52	--	1.97	2.09	1.74	1.73
321-18BL	--	1.56	--	1.60	1.90	1.83	1.75
321-19A	--	1.53	--	2.03	1.96	1.89	1.83
321-19B #1	.75	--	3.27	1.58	1.78	1.49	1.49
321-19B #2	--	1.32	--	1.69	1.61	1.61	1.55
321-19BL	--	1.40	--	2.15	1.63	1.64	1.55

TABLE 13   Resistivity vs. Pyrolysis Temperature

Ω-cm($\times$10)

Sample #	800°C	900°C	1000°C	1577°C	1800°C	2000°C
318-59 #1L	--	--	.499	.102	.083	.110
318-59 #2L	--	--	.522	.099	.081	.060
318-60L	--	--	.523	.0108	.016	.170
321-11L	--	--	.643	.116	.120	.120
321-11CL	--	--	.471	.098	.090	.170
321-12L	--	--	.542	.148	.120	.06
321-13 #1L	--	--	.506	.120	.170	.100
321-13 #2L	--	--	.521	.106	.160	.110
321-13 #3L	--	--	.490	.111	.110	.110
321-15 #1	--	.143	.014	.0302	.015	.015
321-15 #2	.448	--	.029	.0319	.015	.015
321-15L	.324	--	.110	.115	.170	.110
321-16A	.279	--	.014	.029	.015	.015
321-16AL	.366	--	.170	.089	.120	.100
321-16B	.445	--	.030	.0328	.017	.017
321-17B	--	.083	.080	.0357	.018	.018
321-18A	.238	--	.047	.0333	.017	.017
321-18B #1	.611	--	.059	.0334	.016	.016
321-18B #2	.302	--	.03	.0325	.016	.016
321-18BL	.374	--	.160	.114	.110	.110
321-19A	.317	--	.031	.0332	.017	.017
321-19B #1	--	.171	.017	.0368	.018	.018
321-19B #2	.302	--	.03	.0325	.016	.016
321-19BL	.355	--	.150	.081	.110	.110